Environment, Development and Sustainability
https://doi.org/10.1007/s10668-024-05140-0

Resource assessment and techno-economic analysis of solar pv integrated hybrid off-grid power generation system: a case study of Krishnanagar, India

Dipankar Pramanick[1] · Jitendra Kumar[1] · Pankaj Kumar[1] · Himanshu Sharma[1]

Received: 28 June 2022 / Accepted: 11 June 2024
© The Author(s), under exclusive licence to Springer Nature B.V. 2024

Abstract
Integrating renewable energy resources with conventional sources offers a viable option for supplying electricity to remote regions of India, addressing the challenge of inconsistent grid power availability. The study intends to assess the efficacy of solar PV array by estimating several performance metrics, demonstrating the potential for deploying solar PV technology at Krishnanagar located in the eastern part of India and designing a solar PV integrated power generation system (IPGS) by carrying out a comprehensive techno-economic analysis specific to the region. Under the climatic conditions of the aforementioned region, the solar PV system exhibits an annual average Performance-ratio (PR) of 77.50% and a Capacity-factor (CF) of 16.78%. The design and optimization of the IPGS are conducted employing the HOMER Pro application. The obtained result depicts that combining a 12.4 kW PV system, a 6.3 kW diesel generator (DG), a 19 kWh battery energy storage system (BESS) and a 4.83 kW bi-directional converter system (BCS) for a load of 30.39 kWh/d provides the best outcome in terms of least cost-of-energy (COE) and net-present-cost (NPC), while minimising carbon emissions and attaining the maximum renewable fraction (RF). The COE and NPC of the optimal IPGS design are obtained as 0.248 $/kWh and $35,627.85 respectively, with a RF of 96.66%. The carbon emissions obtained from the proposed system is only about 2.5% compared to the DG only configuration. Moreover, the NPC and COE get reduced by 76.4% when compared with DG-only systems. Finally, to further validate the suitability of the proposed system at the considered location, a unique multi-dimensional sensitivity analysis is carried out depicting the variation in COE by varying various parameters that influence power generation and economics.

Keywords Performance indices · Temperature · Solar PV · Cost of energy · Krishnanagar

List of symbols

Y_{PV}	Solar PV rated capacity in kW
f_{pv}	Solar PV derating factor in percentage
P_{PV}	Solar PV output power

✉ Dipankar Pramanick
dipankar.dipz@gmail.com

[1] Department of Electrical and Electronics Engineering, SRM Institute of Science and Technology, Delhi-NCR, Uttar Pradesh, Delhi 201204, India

α_p	Power temperature co-efficient in per ◦C
T_{cr}	Cell temperature of solar PV at standard test condition in ◦C
T_c	Cell temperature of solar PV in ◦C
G_r	Solar radiation incident at STC in kW/m^2
G	Solar radiation incident in kW/m^2
η	Efficiency of solar PV in percentage
τ	Transmittance of solar PV in percentage
U	Co-efficient of heat transfer to the surroundings in kW/m^2/°C
α	Absorptance of PV array in percentage
G_{NOCT}	Solar radiation at NOCT in kW/m^2
E_{AC}	Solar PV AC output in kWh
$E_{AC\ monthly}$	Monthly solar AC output in kWh
E_{DC}	Solar PV DC output in kWh
$E_{DC,\ monthly}$	Monthly solar PV DC output in kWh
$T_{c,\ NOCT}$	Solar PV nominal operating cell temperature in °C
T_a	Ambient temperature in ◦C
$T_{a,\ NOCT}$	Ambient temperature under nominal operating cell temperature in °C
μ	Bi-directional converter efficiency in %
Y_{array}	Solar PV Array yield in h/d
$Y_{reference}$	Solar PV Reference yield in h/d
Y_{final}	Solar PV final yield expressed in h/d
Y_{SL}	System loss in h/d
Y_{CL}	Array capture loss in h/d
P_T	Total power generated from whole system in kWh
P_R	Renewable energy power in kWh
N	No. of observation
Predicted	Predicted value
Obtained	Obtained value
$C_{yearlytotal}$	System's overall annualized cost in $/yr
I	Actual interest rate in percentage
$R_{Project}$	Project life time in year
E_{Served}	Annual electrical load served in kWh/yr
$H_{t,\ daily}$	Daily in-plane solar irradiance in kWh/m^2
CRF	Capital recovery factor

1 Introduction

The progress of any country directly depends on the advancement of its remote areas. The use and generation of energy play a vital role in developing remote areas, especially in India. These remote areas are often affected by frequent power cuts, which pose a substantial barrier to the economic progress of the nation. Thus, ensuring the provision of reliable electricity of high quality in remote areas is imperative for fostering economic progress and enhancing the standard of living for inhabitants (Vendoti et al., 2021). The primary reason for the energy shortfall in remote regions is the lack of utility grid expansion. This challenge can be overcome by designing an integrated power generation system (IPGS) which incorporates renewable energy sources with conventional ones (Goel & Sharma, 2019). This system provides continuous, high-quality, sustainable power to remote areas while

generating eco-friendly energy, thereby reducing global warming and addressing the fossil fuel crisis through decreased reliance on fossil fuels and increased utilization of renewable resources (Kazem et al., 2017).

Recent studies reveal that reducing CO_2emissions can reduce temperature hikes attributed to global warming by 2 °C/year (Vivas & De las Heras et al., 2018). Furthermore, the rapid growth in population significantly escalates energy demand, which is mainly fulfilled by conventional energy sources. According to the report published in the World Energy Outlook 2018 it is anticipated that by 2040, global energy requirements will rise by 30% compared to the current demand (International Energy Agency (IEA). Global shifts in the energy system in world energy outlook 2017). If this increase in energy demand is met by conventional sources, it could have catastrophic consequences for the world and future generations. As a result of these challenges, there is a current global trend towards power generation using renewable sources, for their readily available nature and eco-friendly characteristics. (Sun et al., 2021).

However, renewable resources like wind and solar cannot directly fulfill the energy demand due to their reliance on climatic and weather conditions, which are inherently unpredictable. To overcome this challenge, it is imperative to integrate renewable sources with conventional sources along with storage mechanisms to ensure a dependable energy supply for consumers (Sharma & Goel, 2016).

In India, a substantial share of electricity production depends on traditional sources. According to the report published by the Central Electricity Authority of India, conventional sources account for roughly 88% of electricity generation, while renewable sources contribute approximately 11% (Central electricity authority & executive summary on power sector, 2021). Nevertheless, India has made substantial progress in transitioning to renewable energy sources, doubling its generating capacity through renewable resources over the last five years. Globally, India ranks fifth in solar energy capacity and fourth in wind power capacity (Initiatives achievements & Gov, 2017). The annual solar potential in India exceeds 5000 trillion kWh, with most regions receiving an average per day influx of solar radiation in the range of 4 to 7 kWh/m^2 (Government of India, 2021).

Moreover, data from the National Institute of Solar Energy indicates that solar power capacity of the country is estimated to be 750 GWp. To exploit this immense solar power potential, the Indian administration has introduced several strategies including the bundling initiative, central public sector undertaking program, viability gap funding scheme and the solar park project (MNRE Annual Report, 2020). Additionally, in response to climate change concerns and to mitigate global warming, the Indian government has established a goal of generating 500 GW power utilizing renewable resources by 2030. This ambitious goal includes targets of 140 GW from wind energy and 280 GW from solar energy (Press Information Bureau www.pib.gov.in 2023).

Thus, solar photovoltaic-based IPGS not only help in meeting escalating energy demand but also reduces the reliance on fossil fuel-based energy generation, particularly in regions with limited access to high-quality uninterrupted power supply and where expansion of utility grids is not feasible (Sambhi et al., 2022). The remote regions of eastern India are facing a significant energy shortage problem attributed to the lack of access to utility grid-power. Nearly one-third of households in the area remain without access to power, posing a substantial barrier to the socio-economic progress of the region (Power scenario in West Bengal, 2023). Moreover, the region anticipates a surge in peak demand by about 35%, while the conventional generation capacity stands at 10.7 GW in contrast to the national electric grid capacity of 382 GW, highlighting the need for an alternate power generation approach (Power for All West Bengal 2023). Consequently, the emergence of a hybrid

model based on solar PV presents a viable alternative to bridge the energy gap, mitigate energy shortfall issues, and simultaneously reduce green-house gas emissions.

Therefore, the proposed study focuses on assessing the effectiveness of solar photovoltaic-based IPGS located at Krishnanagar within the eastern part of India. The proposed study aims to determine a wide range of performance metrics of a solar PV array under the local climate and compare them with those reported in existing publications to justify the feasibility of solar PV deployment in the region. Additionally, various techno-economic aspects of the solar PV-based hybrid model have been meticulously analyzed to elucidate its significance in the region. Furthermore, performance analysis has been conducted, taking into account numerous system uncertainties and their influence on system economics and energy generation to rationalize the system's viability.

The primary focus of the present work is outlined as follows:

- To validate the feasibility of PV array deployment in a remote region of eastern India by evaluating performance indices of solar photo-voltaic array
- To validate the use of integrated power generation systems incorporating solar PV by conducting a thorough techno-economic analysis.
- To validate the efficacy of the proposed configuration by performing a unique multi-dimensional sensitivity analysis.
- To further substantiate the feasibility of the proposed configuration through an in-depth comparative analysis of the proposed system with the existing systems reported in the literature.

The article is organized into 11 sections; Sect. 1 includes the introduction, while Sect. 2 offers a thorough review of the literature. The meteorological and load estimation of the study location are discussed in Sect. 3. A detailed methodology using HOMER Pro has been presented in Sect. 4, while the specifications of components forming an IPGS design are outlined in Sect. 5. The study's problem formulation is covered in Sect. 6. Section 7 presents the study's findings and discussions. A comparison between the proposed and the base system is provided in Sect. 8, followed by limitations and implication policies of the study in Sect. 9. Section 10 summarizes the conclusion of the proposed study, and finally Sect. 11 offers recommendations and future work.

2 Literature survey

As global energy consumption continues to surge at a rapid pace, reliance solely on traditional sources proves insufficient to satisfy the escalating demand for energy. Furthermore, this dependence on conventional sources amplifies the consumption of fossil-fuels and contributes to the release of harmful gases, thereby adversely impacting the environment (Few et al., 2022). In light of these challenges, there has been a significant shift in the global energy framework towards the adoption of renewable energy resources. Consequently, researchers around the world have increasingly directed their efforts towards the advancement of energy generation systems based on renewable resources.

In that context, several researchers around the globe have explored various renewable-based hybrid models to generate power in energy-scarce regions. The incorporation of renewable sources relies solely on the potential existence of the resources at the specified location. In the past, scholars predominantly concentrated on assessing the efficiency

of grid connected power generation systems based on renewable energy (Adaramola & Vågnes, 2015; Attari et al., 2016; Ayompe et al., 2011; Fotis et al., 2022; Kumar & Kumar, 2022; Kumar et al., 2019 Jul; Kymakis et al., 2009; Lima et al., 2017; Malvoni et al., 2017; Mondol et al., 2006; Mpholo et al., 2015; Padmavathi & Daniel, 2013; Pawar & Nema, 2018; Pietruszko & Gradzki, 2003; Pujari & Rudramoorthy, 2021; Quansah et al., 2017; Sharma & Chandel, 2013; Sidrach-de-Cardona & Lopez, 1999; Thotakura et al., 2020). However, there has been a gradual shift in the research focus towards renewable energy-based isolated distributed generation due to the impracticality of extending the grid to reach every remote corner (Bhakta & Mukherjee, 2016; Kumar et al., 2018, 2020; Li et al., 2020; Ma et al., 2013; Sambhi et al., 2022b, 2023). In reference (Pawar & Nema, 2018), the author examined the efficacy of the grid-tied solar PV setup installed at the academic institute in India and found that COE obtained for the aforementioned system is lower than the grid-only system. Similarly, Dawood et al. (Dawoud et al., 2015) studied the viability of an integrated model consisting of a solar-DG-battery-converter for a rural region of Egypt. The author concluded that for a load of 48 kW, the system possesses a least COE of 0.139 $/kWh. Likewise, the author in reference (Rahman et al., 2014), analyzed a hybrid model containing two renewable sources, biogas and solar energy for the region of Bangladesh and found that the COE of the model is 0.384 $/kWh for the residential load of 2400 kWh/d. Table 1 presents the recently published works on the optimal renewable energy-based electricity generation systems**,** considering a range of techno-economic parameters.

From the table, it is evident that researchers have developed various hybrid models to fulfill the energy demand cost-effectively, leveraging the availability of energy resources across different locations. Moreover, the optimal hybrid model is designed based on specific technical and economic parameters such as RF, greenhouse gas emissions, unmet load percentage, NPC, and COE. A hybrid power generation system is said to be optimal if it demonstrates high RF, low greenhouse gas emissions, zero unmet load percentage, and minimal NPC and COE. These research findings highlight recent advancements in power generation systems based on renewable energy, particularly focusing on solar energy due to its widespread availability.

Moreover, analyzing the effectiveness of solar PV arrays is crucial to substantiate the feasibility of deploying PV system at specific locations. The technical approach adopted by scholars worldwide to assess the effectiveness of PV arrays involves estimating a wide range of normalized performance metrics such as solar PV generation yields, losses, PR and CF (Attari et al., 2016; Ayompe et al., 2011; Bhakta & Mukherjee, 2016; Jed et al., 2020; Kazem & Khatib, 2013; Kymakis et al., 2009; Malvoni et al., 2017; Mondol et al., 2006; Mpholo et al., 2015; Pietruszko & Gradzki, 2003; Sambhi et al., 2023; Seme et al., 2019; Sharma & Chandel, 2013; Sidrach-de-Cardona & Lopez, 1999) and comparing them against the industry-recommended International Electro-technical Commission (IEC) standard (CODE & P., 1998). Within this framework, researchers examined the performance of PV array by computing different metrics to validate the feasibility of solar PV integrated systems for energy production in Ireland (Mondol et al., 2006), Mauritania (Jed et al., 2020), Italy (Malvoni et al., 2017), Poland (Pietruszko & Gradzki, 2003) and Lesotho (Mpholo et al., 2015). Likewise, performance analysis was conducted for a grid-tied 2.07 kWp PV system in Norway, revealing an energy yield of 1927.7 kWh and corresponding values of PR and CF of PV array were recorded at 83.03% and 10.58%, respectively (Adaramola & Vågnes, 2015). Similarly, the author in reference (Seme et al., 2019), investigated the performance of a grid connected PV array situated in Slovenia, achieving a CF of approximately 12% and a PR of 68%, while also emphasizing the substantial influence of the panel's inclination and azimuth angle on its operational efficiency. Furthermore, in

Table 1 Recent published work on optimal power generation systems based on renewable energy

Period of study	Yea of publication	Author	Main result	Reference
	2018	Duman et al	• Conducted a comparison between two storage elements: hydrogen fuel cell and battery • Evaluated their suitability for a system architecture comprising wind, solar, DG, and a converter • Concluded that battery storage exhibits economic viability	Duman & Güler (2018)
	2018	Gökçek et al	• Designed a PV-wind-battery-converter system • Developed to serve a reverse osmosis plant in coastal regions of Turkey • Achieved a 90% renewable penetration • Noted a COE of 0.308 $/kWh	Gökçek (2018)
	2019	J Kumar et al	• Investigated demand response strategy for a grid-tied solar PV setup in the northern region of India • Observed that shifting non-essential loads during peak demand, resulted in a reduction of NPC and COE for the system	Kumar et al. (2019)
2018–2019	2019	Das et al	• Investigated the impact of dispatch strategies (Load Flow, Combined Dispatch, Cycle Charging) on a solar PV-diesel generator hybrid system • Found that COE remains comparable across strategies, ranging from 0.31 to 0.33 $/kWh • LF strategy shows highest RF of 80%	Das & Zaman (2019)
	2019	Bagheri et al	• Designed a hybrid model for an urban region in Canada • Model includes wind, solar, biomass, natural gas, and battery components • Concluded that NPC and COE for the renewable sources (solar-wind-biomass) are three times lower than those of the solar-wind model	Bagheri et al. (2019)
	2020	Salameh et al	• Examined the effect of tracking system on hybrid systems (Solar PV-DG-Battery-Converter) in the region of Khorfakkan, UAE • Studied Dual-Axis (DA), Continuous Vertical Axis (CVA) and Continuous Horizontal Axis (CHA) tracking systems for solar PV panels • Concluded that Dual-axis (DA) tracking is the optimal option with highest RF and lowest COE	Salameh et al. (2020)
	2020	Miao et al	• Designed a hybrid system for a typical household in the United Kingdom • Components include Wind, Biogas Generator, Battery, and Converter • Configured to fulfil both heating and electric demands • Determined the NPC and COE of the hybrid model at $14,507 and 0.588 $/kWh, respectively	Miao et al. (2020)

Table 1 (continued)

Period of study	Yea of publication	Author	Main result	Reference
2020–2021	2021	Sawle et al	• Examined the suitability of an integrated system for meeting an energy demand of 898 kWh/d in a remote region of Western India • Components include Solar, Wind, Hydro, Diesel Generator, Battery, and Converter • Obtained COE, NPC and RF of the system as 0.916 $/kWh, $831,217 and 81.2%, respectively	Sawle et al. (2021)
	2021	Jeyasudha et al	• Investigated the performance of a hybrid system • Assessments based on RF, annual unmet load percentage, NPC and COE • Observed that the PV-Wind-Bio gasifier-Converter-Battery system exhibits the best result in terms of RF • Found that the PV-Bio gasifier-Converter-Battery system demonstrates the most favourable response with the least NPC and COE	Jeyasudha et al. (2021)
	2021	Awad et al	• Rooftop Photovoltaic (RTPV) system designed for an institute building in Egypt • Employed Particle Swarm Optimization (PSO) for optimal sizing of RTPV • Development and examination of two load forecasting models: medium-term and long-term • Results demonstrate economic feasibility and effective fulfillment of dynamic load demand by RTPV	Awad et al. (2022)
	2022	P Kumar et al	• Analyzed an integrated system comprising Biomass-DG-Battery-PV-Converter for a remote rural region in Eastern India • Considered a load of 880.74 kWh/d for the evaluation • Obtained COE of 0.222 $ /kWh and NPC of $0.922 million • Concluded that the results demonstrate the economic feasibility of the system in the specified region	Kumar et al. (2022)
	2022	Nassar et al	• Proposed a Hybrid-Renewable-Energy-System (HRES) comprising Solar PV, Biomass and Wind • Initial investment for the system is $323 million • The HRES generates 389 GWh annually with 4.57% excess energy generation • Estimated COE for the system is 0.313 $/kWh	Nassar et al. (2022)
2022–2023	2022	Ameur et al	• Compared three solar PV cell technologies: monocrystalline Si-PV, polycrystalline Si-PV, and amorphous Si- PV • Comparative analysis carried out under the climatology of Infrane • Concluded that polycrystalline Si-PV exhibited favourable results in terms of degradation rate, PR, and economic aspects	Ameur et al. (2022)

Table 1 (continued)

Period of study	Yea of publication	Author	Main result	Reference
	2023	Sambhi et al	• Investigated electricity and hydrogen production utilizing renewable resources • Findings indicate that for an electric power consumption of 400 kWh/d, the COE is 0.408 $/kWh • Additionally, for hydrogen production of 10 kg/d, the cost is $16.6/kg	Sambhi et al. (2023)
	2023	Alsharif et al	• Examined the impact of dust accumulation on solar panel efficiency • Conducted experiments to measure the efficiency degradation due to dust deposition • Found that electrostatic cleaning resulted in maximum efficiency, reaching 100%, when the dust concentration was approximately 1 g/m2	Alsharif et al. (2023)

reference (Mehta & Basak, 2020), the author compared results utilizing data collected from various databases and identified a degree of uncertainty in the obtained results.

Furthermore, scholars considered various aspects that impact the power output of solar PV arrays, besides evaluating their performance indices. In (Abdul-Ganiyu et al., 2021), the author compared the performance of conventional PV systems with thermal water-based PV (PVT) and found that for large-scale grid-connected systems, conventional PV is the preferred option. Similarly, in reference (Kabeel et al., 2019), the authors conducted a comparative analysis involving three cooling methods for PV systems, namely, water-based cooling, air-based cooling, and a blend of both, in the presence of a reflector and found that water-based cooling technology yielded the optimal results. In another study (Padmavathi & Daniel, 2013), the investigation explored the impact of inverter loss and grid failure on the operation of a 3MWpsolar PV array situated in the southern region of India. The results demonstrate a disproportionate decrease in PR as grid failures and inverter losses escalate. Likewise, the author in reference (Ma et al., 2013) examined the influence of cell temperature on the output power of PV arrays, observing a decline in the system's output power as PV cell temperature increases**.** Additionally, reference (Kumar et al., 2021a) explored a power controller scheme utilizing fuzzy logic for distributed generation systems with inverters and concluded that the control scheme exhibits better voltage and frequency control compared with conventional PI controller schemes.

Further, researchers utilized various software and data gathering tools such as PVWATTS (Thotakura et al., 2020), PVsyst (Photovoltaic systems) (Sharma & Chandel, 2013), SAM (System Advisor Model) (Malvoni et al., 2017), HOMER Pro (Hybrid-Optimization of Multiple-Energy-Resources) (Bhakta & Mukherjee, 2016), Meteonorm (en) (Allouhi et al., 2016), PVGIS (Photovoltaic Geographical Information System) (Thotakura et al., 2020), and PDAV (Power Data Access Viewer) (Kumar et al., 2020) to assess the effectiveness of PV arrays. For the proposed study, HOMER Pro software is being employed. This software is extensively used by researchers worldwide (Aziz et al., 2020; Gökçek, 2018; Jeyasudha et al., 2021; Kumar et al., 2022; Kumar et al., 2019 Jul; Shahzad et al., 2017). It offers a more user-friendly interface compared to other simulation software tools such as PVsyst and PVSOL. In a comparison among three software options- PVsyst, PVSOL, and HOMER Pro it was found that HOMER Pro demonstrates optimal results in terms of PR and energy output for solar PV plants. HOMER Pro utilizes a heuristic search algorithm, aiming to provide the best possible solution based on input parameters. This approach often yields practical and efficient solutions. However, it's important to note that HOMER's optimization approach may not explore all potential solutions exhaustively, as some other software might which employ primary and secondary algorithms to fine-tune their results. As such, HOMER Pro requires considerably lesser time to provide results, making it a valuable option when time is a critical factor (Saiprasad et al., 2018; Souza Silva et al., 2020).

Therefore, based on energy resource availability at different locations, the scholars designed various hybrid models to meet the load at the optimal low cost. It is clear from the extensive literature survey that integrating renewable energy sources with conventional systems can mitigate the problem of intermittent power supply in rural areas. Digitalization enables peer-to-peer node connections, facilitating the decentralization of renewable energy and enhancing energy efficiency within society (Esposito & Brahmi, 2023). Furthermore, recent technological advancements have paved the way for a smooth transition towards sustainable energy models (Esposito et al., 2023).

However, as researchers worldwide concentrate on developing alternative power generation models utilizing renewables to cater the energy crisis in remote regions, certain issues

remain unaddressed. These include choosing energy sources according to the performance of resources at the specified location. Additionally, the implications of renewable energy penetration on system economics have been rarely explored by scholars. Furthermore, a multi-dimensional approach to sensitivity analysis has yet to be pursued. The present study aims to address these assessments, aiming to consolidate the use of renewable integrated power generating models for electrifying remote areas. Moreover, performance analysis has been conducted, considering numerous system uncertainties and their effect on system economics and energy generation, to further rationalize the system's viability.

The novel contributions from the authors in the proposed study are listed below, which provide a viable potential alternative for delivering improved quality reliable power to remote locations.

- A unique approach for designing a hybrid model based on performance assessments of energy resources for the given location.
- The impact of diverse naturally occurring uncertain variables on the system's performance has been analyzed using a unique three-dimensional approach to assure the system's robustness.
- Examined the effect of the RF on the system's performance in terms of economics.

Thus, the current study presents a unique approach for analyzing a self-sustained solar PV based hybrid model and justifies its worth for rural electrification, ensuring reliability and sustainability of power supply.

3 Meteorological condition and energy demand estimation

The proposed study is undertaken for Krishnanagar, located in the Nadia district of southern West Bengal as shown in Fig. 1. The region lies in the eastern part of India, with its exact location at 23.4013°N latitude and 88.5021° E longitude. As per the

Fig. 1 Map showing study area

census of 2011, the area comprises 12,963 residents, consisting of 6667 males and 6296 females, residing in approximately 3043 households (District census handbook Nadia series-10 Part XII-a, village & town directory., 2011).

The region experiences frequent power outages, and expanding utility-grid power infrastructure is challenging, leading to a significant energy shortage that has hindered economic growth of the region. However, the area benefits from ample solar radiation, attributed to its location along the Tropic of Cancer. This serves as the foundation for analysing solar PV performance and integrating solar resources with traditional sources to address the energy deficit.

Meteorological and climatic data for the chosen site were acquired through the Power Data Access Viewer (PDAV) application provided by NASA (Multiple data access option, National Aeronautics & Space Administration, 2021**).** The site experiences distinct seasonal changes, with summer spanning March to May, followed by the monsoon period from June to September, and finally, winter and mist season observed from October to February. Figure 2 shows clearness index (CI) and global horizontal irradiance (GHI) of the considered site. GHI fluctuates between (4.09—6.17) kWh/m^2/day, highlighting substantial variations in solar radiation. Higher GHI values are recorded in the summer months, averaging a daily radiation of 5.94 kWh/m^2, contrasting with a lower average of 4.39 kWh/m^2 per day, observed during the monsoon season. Similarly, the CI varies from 0.394 to 0.631, reflecting variations in atmospheric clarity that impact solar radiation. The higher CI values with an average of 0.618 observed in the winter months and lower value of CI is observed in the monsoon months, with a mean value of 0.442. Both GHI and CI exhibit lower values during the monsoon season. The overall annual average GHI and CI for the region are 4.79 kWh/m^2/day and 0.53, respectively.

In addition to solar radiation, solar PV cell temperature and ambient temperature have a significant impact on determining solar PV power output (Hafez et al., 2020). Figure 3 shows solar PV cell and ambient temperatures of the region. The yearly mean ambient temperature for the region is 26.04 °C. Higher values of ambient temperature obtained in the summer months of the region with an average temperature of 31.52 °C and lower values observed during winter months with an average of 19.97 °C. Correspondingly, annual average solar PV cell temperature in the region is obtained as 32.38 °C, with higher values obtained in the summer months (37.39 °C) and lower values recorded in

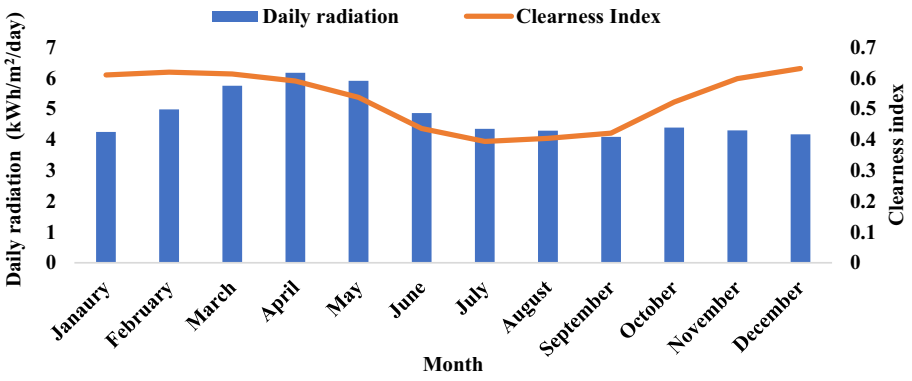

Fig. 2 GHI and CI of the considered site

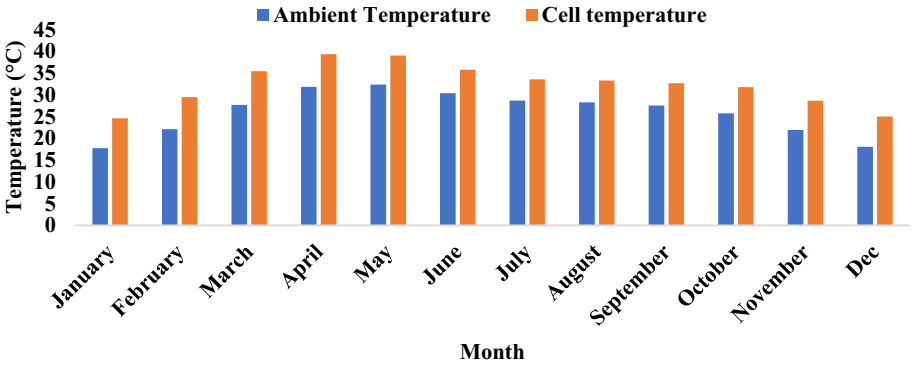

Fig. 3 Ambient temperature and Solar PVcell temperature of the considered site

the winter months (26.93 °C). It is evident from the figure that the months with higher ambient temperature shows higher value of solar PV cell temperature.

The load estimation of the considered site has been found by an onsite field survey based on questionnaire. The survey was carried out for 10 households in the month of May. It was found that the majority of essential electric load requirements are for the appliances, like overhead fans, television, water pump motor, light etc. The daily energy requirement for 10 households at the selected site was obtained as 30.39 kWh. This estimation is crucial as it provides insights into the energy consumption patterns. The assessment of energy requirement of the considered location shows that maximum energy is being consumed by ceiling fan, which operates nearly 12 h a day resulting in 18 kWh of energy. LED bulb consumes 6 kWh of energy which operates for nearly 10 h a day. Further, 40 min time required by 0.5 hp motor to fill a water tank of 1000 L, which suggests around 2.5 kWh of energy consumptions. Detailed load estimation of ten household is shown in Table 2.

The load profiles on a daily and monthly basis at the considered location are shown in Figs. 4 and 5, respectively. It depicts that the highest power consumption occurs in the evening, with an average demand of 3.72 kW, reaching peak of 5.64 kW, attributed to the simultaneous use of all appliances. On the contrary, energy consumption is lower from midnight to early morning, with an average demand of 0.25 kW. Additionally, energy usage increases during noon due to increased usage of ceiling fans. Correspondingly, maximum energy consumption occurs during the summer season (3.48 kW) and in the months

Table 2 Load estimation

Component	Quality	Watts	Hours	Total load (Wh)
LED	6	10	10	600
Water pump motor	1	373	0.67	249.91
Television	1	120	3	360
Phone Charger	1	5	6	30
Overhead Fan	2	75	12	1800
Energy demand for one household (Wh)				**3039.91**
Energy demand for one household (kWh)				**3.039**
Energy demand for 10 household (kWh)				**30.39**

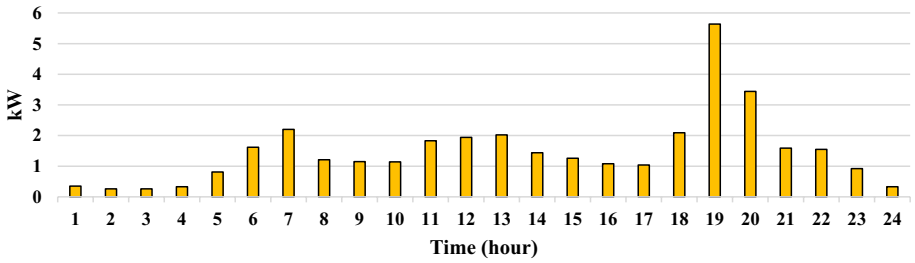

Fig. 4 Residential load profile on a daily basis for the selected site

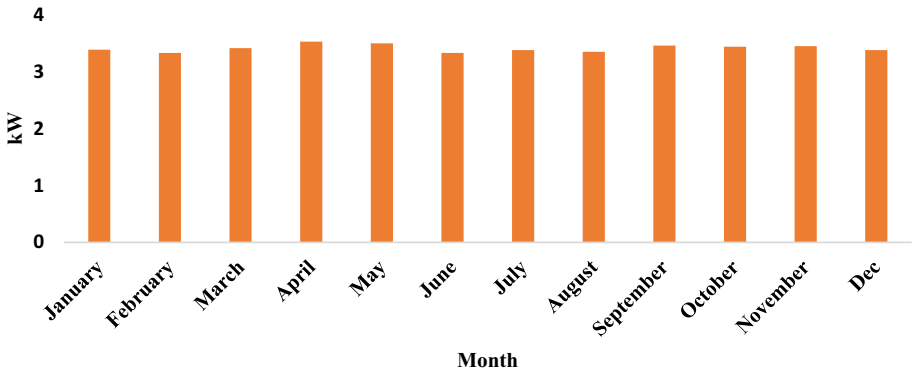

Fig. 5 Residential load profile on a monthly basis for the selected site

of October and November (3.44 kW), attributed to the festive season in the region. On the other hand, minimal energy consumption occurs during monsoon seasons, with an average load demand of 3.35 kW.

4 Methodology

The methodology broadly involves three stages: assessment, simulation, and analysis. The block diagram in Fig. 6 illustrates the proposed study using HOMER Pro application, as shown. In the first stage, various necessary assessments, including load and resource assessments, have been performed. In the second stage, simulation is conducted through HOMER. Finally, in the last stage, various analyses are carried out based on the simulation outcomes.

In the resource assessment, variables such as solar radiation and temperature of the designated site are taken into consideration, given their direct influence on solar PV power generation. Following the resource assessment, load demand estimation is conducted through an infield survey of residential load in the region. For simulation, real-time cost information for various components involved in the IPGS design, along with load specifics for the considered site are incorporated into the HOMER Pro application. The study also includes the consideration of temperature's impact on solar PV array. The time series data obtained from simulation is being analyzed to estimate the performance metrics of

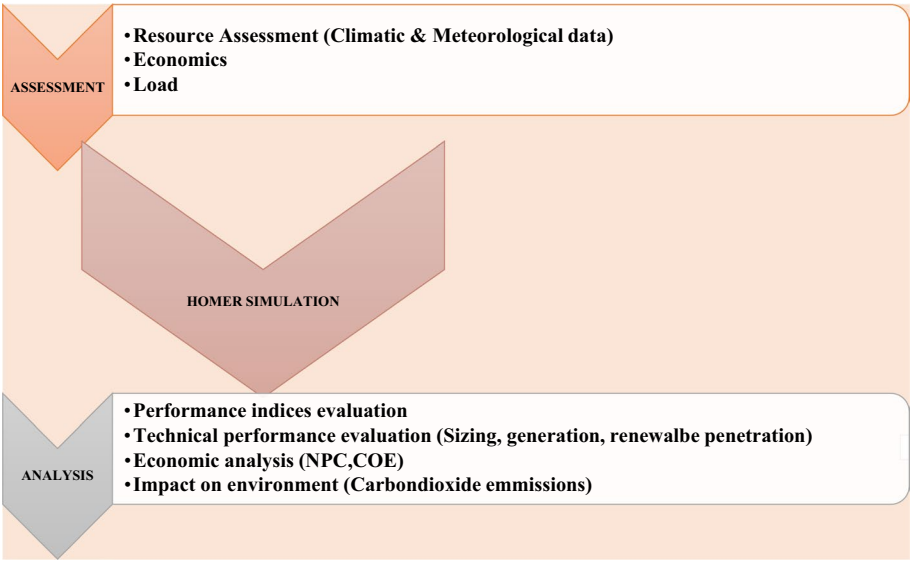

Fig. 6 Block diagram representation of HOMER software

the solar PV system at the selected site. Finally, various techno-economic analyses of the integrated power generation model are conducted. HOMER Pro software facilitates the feasibility of various system architectures. The assessment relies on critical metrics, namely NPC and COE, which play pivotal roles in ranking different configurations.

Moreover, COE emerges as a key determinant of system viability, particularly in remote areas where consumers prioritize economic considerations. The close interdependence between COE and NPC is evident, as NPC relies heavily on the investment incurred during project implementation. Additionally, optimal sizing of system components based on load requirements is vital for cost minimization. Furthermore, addressing current environmental concerns by minimizing pollutants emitted by the system is essential for achieving sustainable goals. The emphasis on renewable penetration, representing the proportion of energy derived from renewable sources, is pivotal for mitigating harmful gas emissions. The proposed integrated power generation system (IPGS) is designed to be optimal, characterized by higher renewable penetration, lower carbon emissions, and minimized NPC and COE. This research methodology ensures a comprehensive evaluation of the proposed system, focusing on key techno-economic parameters aligned with sustainability and efficiency goals.

5 Components of integrated power generation system

The major components of IPGS consist of a DG, battery storage system (BESS), solar PV, and bi-directional converter system (BCS). A schematic representation of the IPGS is illustrated in Fig. 7. The PV system operates by harnessing solar energy and transforming it into electrical energy. The DC electrical energy produced from PV array is transformed to AC using a converter. Further, DG and battery storage system are included in the system to provide reliable power supply. It is important to note that there are certain assumptions

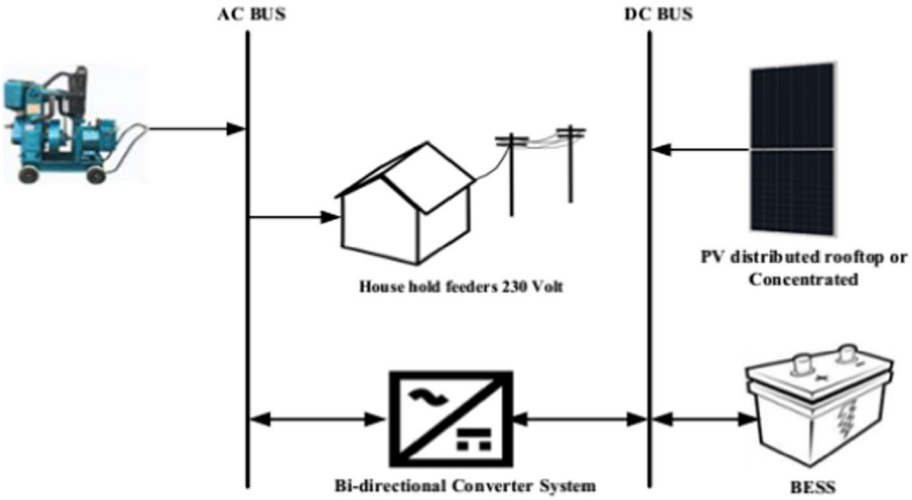

Fig. 7 Schematic diagram of IPGS

associated with each component, that are considered, while designing and optimizing IPGS model. For instance, the minimum-load-ratio for the DG is considered as 25% (Sambhi et al., 2023), providing a baseline for assessing its performance under varying load conditions. The baseline level for the SOC of the BESS is assumed to be 20% (Kumar et al., 2021), reflecting the lower limit to which the system's is allowed to deplete. Ground reflectance, a crucial factor in PV systems is assumed to be 20% (Bhakta & Mukherjee, 2017), influencing the efficiency of solar energy absorption. Converter efficiency of 95% has been considered for the study, accounting for energy losses in conversion process (Pujari & Rudramoorthy, 2021). Moreover, the study incorporates a minimum load criterion for the site, with 20% random step time variability and 10% day-to-day, capturing the dynamic nature of energy demand (Kumar et al., 2021). These considerations collectively contribute to a comprehensive and realistic evaluation of IPGS under diverse operational conditions.

5.1 Solar PV array system

Out of all renewable resources, solar power is the most prevalent choice for generating electricity in distant parts of the country due to its abundant supply. Recognizing its significance, the Indian government has implemented several visionary initiatives aimed at promoting the adoption of solar resources and enhance the lives of its citizens. The Pradhan Mantri Kisan Urja Suraksha evam Utthan Mahabhiyan (PM-KUSUM) initiative is one such endeavour targeted to empower farmers, offering financial assistance for establishing solar power plants on their barren lands (PM-KUSUM (Pradhan Mantri Kisan Urja Suraksha evamUtthaanMahabhiyan 2023). This initiative not only enables farmers to create a sustainable source of income but also contributes to the country's clean energy objectives. Apart from this, the Pradhan-Mantri-Ujjwala-Yojana, which initially focused on providing clean cooking fuel (LPG) to rural households, has been expanded to include the distribution of solar cook stoves. This initiative aims to reduce the dependence on traditional cooking methods, improve indoor air quality, and advocate for the utilization of renewable energy for daily cooking needs (Ministry of Petroleum Natural Gas, 2023).

Further, the smart cities mission includes provision for integrating solar energy source to enhance energy efficiency and sustainability in urban areas (Ministry of Housing & Urban Affairs, 2023). Additionally, numerous local initiatives have emerged up across the country, supported by the government, to encourage communities to harness solar energy for their needs (Ministry of New & Renewable Energy, 2023). Furthermore, to support standalone solar PV integrated power generation systems, the Indian government introduced the Atal Jyoti Yojana (AJAY) scheme, with a specific focus on deploying solar LED streetlights in areas lacking grid connectivity (Information & Bureau, 2023). These collective efforts signify a transformative shift towards a greener and more sustainable energy landscape in India. Moreover, in the context of the Integrated Power Generation System (IPGS), solar power is crucial for addressing energy needs. Thus, making it an integral part of the hybrid model design. The solar PV array generates power in the form of DC, with its output directly influenced by the solar irradiance and temperature conditions at the site. Figure 8 illustrates a schematic of a solar PV system, emphasizing its crucial role in the broader context of the energy system.

The standard expression for estimating the power generation of a PV system is provided by Eq. (1) (Kazem & Khatib, 2013)

$$P_{pv} = Y_{pv} f_{pv} \left(\frac{G}{G_r} \right) \left[1 + \alpha_p \left(T_{c\_} T_{cr} \right) \right] \tag{1}$$

During daylight hours, the cell temperature surpasses the ambient temperature owing to solar radiation exposure. Conversely, at night, the PV cell temperature aligns with the ambient temperature in the absence of direct sunlight. For the analysis, the value of τα is considered as 0.9(Bhakta & Mukherjee, 2016). Hence, Eqs. (2) and (3) can be used for calculating solar PV cell temperature (Duffie et al., 2020).

$$\tau\alpha G = nG + U\left(T_c - T_a \right) \tag{2}$$

$$T_c = T_a + G\left(\frac{\tau\alpha}{U} \right)\left(1 - \frac{n}{\tau\alpha} \right) \tag{3}$$

However, considering efficiency of solar PV array under no load condition at NOCT equal to zero, the term τα/U can be estimated using Eq. (4).

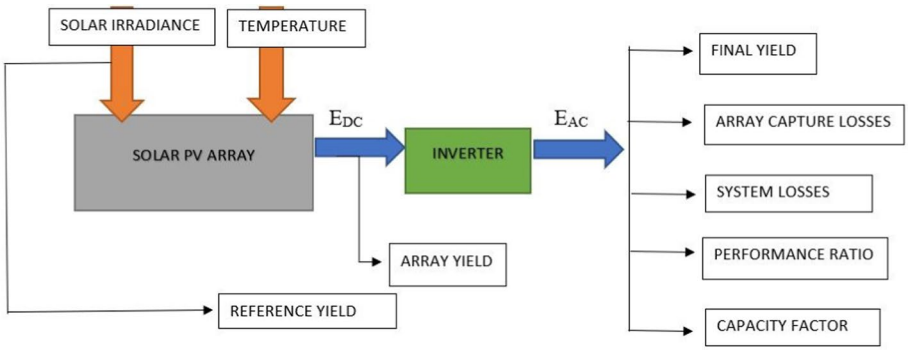

Fig. 8 Schematic of solar PV system

$$\frac{\tau\alpha}{U} = \frac{T_{C,NOCT} - T_{a,NOCT}}{G_{NOCT}} \tag{4}$$

Moreover, considering τα/U as a fixed value and substituting the value obtained from Eq. (4) into Eq. (3) yields a modified equation for the solar PV array's cell temperature, as depicted in Eq. (5).

$$T_c = T_a + G\left(\frac{T_{c,NOCT} - T_{a,NOCT}}{G_{NOCT}}\right)\left(1 - \frac{n}{\tau\alpha}\right) \tag{5}$$

The proposed study utilizes the CSK 290MS All-Black monocrystalline solar PV module by Canadian Solar, chosen for its superior efficiency and durability. It generates more power compared to other solar PV arrays, attributed to the inclusion of rear contact cells with a black frame and black sheet. The initial investment for this solar PV system is $725 per kW, with an annual operational and maintenance expense of $10 per kW (Pujari & Rudramoorthy, 2021). The technical parameters of the solar PV array are presented in Table 3.

5.2 Battery energy storage system (BESS)

The BESS is integrated within the design to ensure continuous and uninterrupted operation of the IPGS. The BESS considered for the design is the Discover 12VRE-3000TF lead-acid battery, chosen for its cost-effectiveness and ease of maintenance. The initial capital investment and replacement expenses for single BESS unit are $410 and $350, respectively, with an annual operation and maintenance expense of $10. The battery has a maximum capacity of 260 Ah (Pujari & Rudramoorthy, 2021). Detailed technical specifications of the BESS are provided in Table 4.

5.3 Back-up system: DG

The challenge of low reliability in hybrid systems comprising solar PV and battery storage acts as a significant barrier to their widespread development. Therefore, integrating DG as a backup unit in the architecture enhances the reliability of the system. In the

Table 3 Technical parameters of solar PV array (Solar & all black CS6K-290MS monocrystalline Canadian Solar module, 2019)

Parameters	Value
Manufacturer	Canadian Solar CS6K-290MS
Rated Capacity at standard test condition (STC)	290 W
Efficiency	17.72%
Derating Factor	88%
Temperature Coefficient	−0.39/°C
Solar incident radiation at STC	1000 W/m^2
PV Cell temperature at STC	25 °C
Ambient temperature at NOCT	20 °C
Nominal Operating Cell Temperature (NOCT)	45 °C

Table 4 Specifications of BESS (Discover Innovative battery solution, 2021)

Parameters	Value
Manufacturer	Discover innovative battery solutions
Nominal Capacity in kWh	3.11
Nominal Voltage in Volts	12
Efficiency in percentage	80
Maximum amount of charge current in Ampere	43
Total internal resistance in mΩ	5
Maximum Capacity (Ah)	260
Lifetime throughput (kWh)	3581.60

proposed study, an auto-size genset DG is used. It automatically sizes itself according to load demand, and HOMER utilizes this capability to optimize system sizing. The software considers an array of factors, including load data, system components, resource availability, economic parameters, lifespan etc. to simulate the system.

Using a search space criterion, HOMER optimizes the size of components, with inputs given in the form of ranges over specific step size. The selection process prioritizes load requirements and economic considerations, offering various feasible system architectures that align with dispatch strategies, namely load flow (LF) and cycle charging (CC) and. These built-in methods, inherent in the software, can be practically implemented using dynamic controllers like PLCs or microcontrollers. Under CC, the DG runs at its rated capacity to fulfil energy requirements and charges the BESS until a specified SOC is reached, efficiently utilizing excess energy. In LF, the system prioritizes solar PV for load demand, adjusting DG operation based on energy surplus or deficit, effectively managing energy resources. Through these criteria, HOMER meticulously determines the optimal DG size, ensuring a reliable solution for peak demand scenarios. Furthermore, given a choice of generator sizes, it selects the smallest one that meets the annual maximum capacity shortage requirement (Lilienthal, 2016a).

The capital and replacement expenses of DG per kW amount to $500, with an O&M cost per operational hour of $0.03. The assumed lifespan of this generator unit is 15000 h (Pujari & Rudramoorthy, 2021). Additionally, the cost of diesel fuel in West Bengal is $1.2 per litre. Figure 9 shows the characteristics curve of the diesel generator. It is observed from the curve that for 1.26 kW of output, consumption of fuel is 0.64

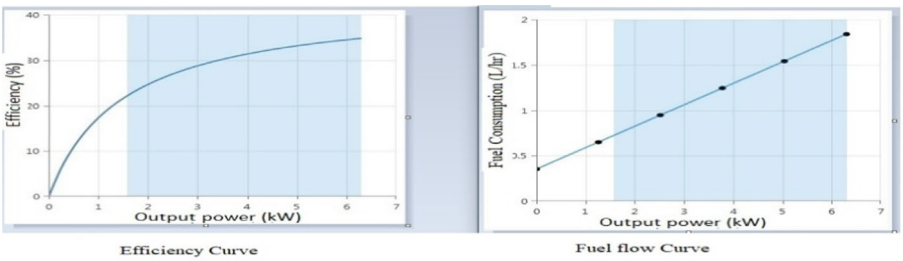

Fig. 9 Fuel Characteristics Curve of DG

L/hr, and for 6.3 kW output, fuel consumed by the DG is 1.83 L/hr. From the curve, the reference generator capacity is measured as 6.3 kW with a coefficient of intercept of 0.055 L per hour per kW of rated value. The slope is obtained as 0.236 L per hour per kW of output (Kumar et al., 2021b). Detailed specifications of DG acquired from HOMER Pro application (Lilienthal, 2016a) are shown in Table 5.

5.4 Bi-directional converter system (BCS)

The system design incorporates this unit, essential for the conversion of power between DC and AC. A generic system converter is chosen for the design, with a capital and replacement cost per kW amounting to $800 and $600, respectively. Additionally, the annual operational and maintenance (O&M) expenses for the converter amount to $5, estimating a lifespan of 25 years (Pujari & Rudramoorthy, 2021).

6 Problem formulation

The main objective of this paper is to determine solar PV potential at the selected location through the assessment of various performance indices**,** as discussed in the subsequent sections. Additionally, the study conducts an in-depth techno-economic assessment of IPGS design using solar PV to investigate the self-sustainability of the model in the considered location. The NPC and COE are two critical measures used to optimize the system layout in economic terms. Moreover, this work intended to design an IPGS system with the highest RF and minimal carbon emissions.

Table 5 Technical details of DG (Sambhi et al., 2023)

Fuel	
Fuel type	Diesel
Intercept of fuel curve	0.352 L/h
Slope of fuel curve	0.236 L/h/kW
Emissions	
NO_x	15.5 g/L of fuel
PM	0.1 g/L of fuel
Fuel sulphur to PM	2.20%
Unburned HC	0.72 g/L of fuel
CO	16.5 g/L of fuel
Properties of fuel	
Density	820 kg/m^3
Lower heating value	43.2 MJ/kg
Sulphur content	0.40%
Carbon content	88%

6.1 Performance indices

In order to determine solar PV array's performance, directives issued under IEC standard 61724 (CODE & P., 1998) &International Energy Agency Photovoltaic Power System (IEA PVPS) task II (Jahn et al., 2000) are followed, recognized by India under the oversight of the Bureau of Indian Standards. To evaluate various performance indices, it is imperative to obtain the power output of the PV system. The DC output obtained from solar PV array is converted into AC energy, considering the efficiency of the converter. Performance indices in solar PV systems encompass a range of parameters that measure the efficiency, output, and losses within the system.

The parameters utilized for investigating the effectiveness of the PV array under these guidelines are the final yield (Y_{final}), array yield (Y_{array}), reference yield ($Y_{reference}$), system loss (Y_{SL}), array capture loss (Y_{CL}), PR and CF. Array yield, a critical parameter, indicates the correlation between the DC energy output generated by a PV array and its rated power, serving as an indicator of the system's DC energy production performance. Conversely, reference yield provides insights into the solar potential at a particular site during a designated time frame, represented as the cumulative horizontal solar radiation compared to a reference irradiance of 1 kW/m^2.

Furthermore, the final yield is determined by the proportion of AC generated energy to the PV array's rated capacity over a specified time-frame. It facilitates comparisons among PV arrays installed at different locations**.** The performance ratio, another essential metric, reveals various losses within the system, such as inverter loss, heat loss, wiring loss, and environmental factors. It denotes the ratio of the final to the reference yield.

Correspondingly, the capacity factor indicates the efficacy of the PV array by comparing actually produced energy by the PV array with the energy that would be produced if the system runs at its fullest capacity for 24 h every day throughout the year. Further, metrics that depicts losses include array capture loss and system loss. Array capture loss highlights the variation between the actual and reference solar radiation, indicating the incomplete capture of solar irradiance by a solar PV array during operation, while system loss reflects the overall losses within the PV system and shows the disparity between array yield and final yield. Table 6 shows the mathematical representation for various performance indices.

Table 6 Solar PV performance indices

Performance indices	Mathematical expressions	References
AC output energy	$E_{AC} = \mu E_{DC}$	Bhakta & Mukherjee (2016)
Array yield	$Y_{array} = \frac{E_{DC,monthly}}{Y_{PVrated}}$	Kymakis et al. (2009)
Reference yield	$Y_{refernce} = \frac{H_{tdaily}}{1kWh/m^2}$	Adaramola & Vågnes (2015)
Final yield	$Y_{final} = \frac{E_{AC,monthly}}{Y_{PVrated}}$	Mondol et al. (2006); Ayompe et al. (2011)
System loss	$Y_{SL} = Y_{array} - Y_{final}$	Ayompe et al. (2011); Kumar et al. (2020)
Array capture loss	$Y_{CL} = Y_{reference} - Y_{array}$	Ayompe et al. (2011); Kumar et al. (2020)
Capacity-factor	$CF = \frac{E_{AC,yearly}}{Y_{PVrated}X24X365}$	Sharma & Chandel (2013); Bhakta & Mukherjee (2016)
Performance-ratio	$PR = \frac{Y_{final}}{Y_{reference}}$	Kymakis et al. (2009)

6.2 Techno-economic analysis

To achieve the optimal IPGS design configuration for the selected site based on economic feasibility, the COE and NPC are being assessed. The configuration with the lowest COE and NPC is considered the most favourable. The NPC and COE for different system configurations are determined by using Eqs. (6) and (7), respectively (Bhakta & Mukherjee, 2017; Kumar et al., 2021b).

$$NPC = \frac{C_{yearlytotal}}{CRF\left(i, R_{project}\right)} \tag{6}$$

$$COE = \frac{C_{yearlytotal}}{E_{served}} \tag{7}$$

The NPC of the system is based on the annualized overall expense of the system, which is determined utilizing the initial capital investment, replacement, operational and maintenance cost of various components included in the IPGS along with fuel prices (if the system contains a DG) over a specific period. Besides these expenditures, the salvage or residual value of the components also impacts the system's cost. The remaining value associated with components after project life is called salvage value, and it is proportional to the remaining life (in years) of components used in the power system. The NPC also influenced by the actual discount rate and project lifetime. Apart from NPC, COE is another aspect that is considered in the proposed study for examining economic viability of the system. The COE represents the per annum overall cost of the system in relation to the electrical load served, encompassing both primary and deferrable loads. In other words, COE stands for the cost of generating electricity per kWh. The cost specifications of various components forming an IPGS are shown in Table 7. In addition to that, RF is another crucial metric that defines the technical feasibility of the system for a given location. With the increase in RF, the system's carbon emission reduces. RF is defined as the portion of energy produced from renewable sources compared to the overall output of the system. Equation (8) expresses the renewable fraction in percentage (Jeyasudha et al., 2021).

$$RF = \frac{P_R}{P_T} \tag{8}$$

The comparison between NPC and COE against the RF serves as a critical evaluation of techno-economic aspects in renewable energy projects. NPC is a comprehensive metric that considers the entire lifecycle cost, encompassing initial investments, operational expenditures, and potential salvage value. It provides a general view of the financial aspects of a

Table 7 Cost specification of components (Pujari & Rudramoorthy, 2021)

Components	Capital expense	Replacement expense	O&M expense	Life	Fuel rate
Solar PV	$725/kW	$725/kW	$10/kW/year	25 years	1.2$/L
DG	$500/kW	$500/kW	$0.03/op hour	15,000 h	
BESS	$410/unit	$350/unit	$10/year	25 years	
BCS	$800/kW	$600/kW	$5/year	25 years	

project, aiding in decision-making. On the other hand, COE offers a per-unit basis for cost, facilitating direct comparisons between different energy sources. It is particularly valuable for assessing the economic competitiveness of renewable projects. In contrast, RF focuses on the environmental dimension, indicating the proportion of energy generation through renewable sources relative to the system's total energy production.

In the context of the proposed study, the significance of cost becomes paramount for the local community. The cost of per capita energy consumption plays a central role in shaping the socio-economic growth of the residents in the remote regions. Furthermore, it's essential to note that the COE is intricately linked to the NPC of the system. Reflecting economic implications at a community level, COE holds local significance, while RF gains prominence on the global scale, representing a crucial metric in the pursuit of sustainability and environmental responsibility.

While NPC and COE are pivotal for financial analysis and decision-making, RF adds a sustainability perspective, ensuring that both environmental and economic factors are considered in the evaluation process. A balanced techno-economic assessment, in this context, involves considering both NPC and COE for financial viability, complemented by RF to measure the project's environmental impact and overall sustainability. Thus, for the proposed study, a detailed analysis based on COE and NPC along with RF is being considered for the selected region.

7 Results and discussion

The site under consideration possesses ample solar resources. Meteorological data, including GHI and ambient temperature, have been obtained over a 22-year period using the PDAV application from NASA, with precise geographical specifications for the region. Solar PV performance is directly affected by solar irradiance, as illustrated in Eq. (1). Conversely, the CI offers insights into the level of solar radiance that reaches a solar panel after penetrating the atmosphere. A higher CI value signifies greater solar energy potential, with values ranging between 0 and 1. Both parameters play crucial roles in determining the power generation of a PV array.

Figure 2 illustrates the GHI and CI values at the considered site. It is evident that daily solar insolation fluctuates between 4.09 and 6.17 kWh/m^2, peaking during April and reaching its lowest point during September. The data reveals a seasonal pattern, with solar irradiation higher during the summer seasons and lower during the monsoon seasons. Correspondingly, the CI value ranges from 0.394 to 0.631, having the maximum value recorded in December and the lowest value in July. Further, there is a notice able decline in the CI value during June, July, and August, aligning the observed monsoon season in the region.

Besides solar radiation, PV cell and ambient temperatures are essential factors in estimating the power generation of solar PV panels, as highlighted within Eqs. (1–5).Furthermore, ambient temperature significantly impacts the temperature of PV cells, which consequently affects the output of solar PV systems. Figure 3 illustrates the ambient and cell temperature of the region. The highest temperature in the region is observed in May, while the lowest occurs in January, averaging 26.02 °C annually. Similarly, the PV cell temperature at the selected site fluctuates between 23.68 °C and 38.36 °C, with the highest and lowest levels obtained in May and January, respectively. Therefore, it is apparent that higher ambient temperatures correspond to elevated solar PV cell temperatures.

The general residential load for the selected area includes essential appliances such as televisions, LEDs, overhead fans, water pump motors, and mobile chargers, as shown in Table 2. Upon estimation, it was determined that the energy consumption for 10 residences in the region amounts to 30.39 kWh/d. Figure 4 and 5 depict the load profiles on daily and monthly basis for the considered location. Notably, the peak energy usage occurs during the (18:00–21:00) hours, aligning with the simultaneous operation of domestic appliances. Subsequently, there is a decline in energy consumption post-midnight, particularly between (01:00—04:00) hours, with an average consumption of 0.25 kWh during this timeframe.

7.1 Evaluation of performance indices

The assessment of the solar PV array's performance involves determining metrics such as array, final and reference yields, CF, PR, system loss and array capture loss. To compute these metrics, the energy outputs (DC and AC) of the solar PV system must be calculated. The PV DC energy production is determined using time-series data obtained from the HOMER Pro software (Lilienthal, 2016b). Subsequently, this energy is converted to AC energy, accounting for a converter efficiency of 95%.

The monthly energy outputs (both AC and DC) of the PV array at the designated site are presented in Table 8. It is noted that the average DC energy output per annum for the site is 52.56 kWh, with the highest DC energy output recorded in March (62.81 kWh) and declining to the minimum in July (40.55 kWh). The reduced DC energy output in July can be attributed to the overcast weather conditions, resulting in a low atmospheric CI. Similarly, the yearly mean AC output of PV array at the site is determined at 49.93 kWh, with the highest AC energy output observed in March (59.67 kWh) and the lowest in July (38.52 kWh). Despite the peak solar radiation occurring in April and December marking the highest CI, the data indicates that the maximum solar PV output is obtained in March. This insight underscores the significant impact of factors such as PV cell and ambient temperatures on solar PV performance.

The DC and AC energy output of PV systems are crucial factors for estimating the PV array's performance indices. Once these values are obtained, the performance indices can be calculated using the expressions provided in Table 6. A comprehensive range of

Table 8 Energy generated by PV array at the considered site (Lilienthal, 2016b; Multiple data access option, National Aeronautics & Space Administration, 2021)

Month	E_{DC} (in kWh)	E_{AC} (in kWh)
January	58.14	55.23
February	61.37	58.30
March	62.81	59.67
April	59.90	56.90
May	53.74	51.05
June	44.41	42.19
July	40.55	38.52
August	41.60	39.52
September	42.51	40.38
October	50.13	47.63
November	56.22	53.41
December	59.36	56.39
Mean	52.56	49.93

Table 9 Solar PV array performance metrics at the proposed location (Lilienthal, 2016b; Multiple data access option, National Aeronautics & Space Administration, 2021)

Month	Y_{array} (h/d)	$Y_{reference}$ (h/d)	Y_{final} (h/d)	Y_{CL} (h/d)	Y_{SL} (h/d)	PR (%)	CF (%)
January	4.69	5.60	4.45	0.91	0.23	79.53	18.56
February	4.95	6.02	4.70	1.07	0.25	78.06	19.59
March	5.06	6.31	4.81	1.25	0.25	76.21	20.05
April	4.83	6.09	4.59	1.26	0.24	75.32	19.12
May	4.33	5.44	4.12	1.11	0.22	75.68	17.16
June	3.58	4.42	3.40	0.84	0.18	77.01	14.18
July	3.27	4.00	3.11	0.73	0.16	77.63	12.94
August	3.36	4.11	3.19	0.75	0.17	77.55	13.28
September	3.43	4.21	3.26	0.78	0.17	77.39	13.57
October	4.04	4.94	3.84	0.90	0.20	77.76	16.00
November	4.53	5.50	4.31	0.97	0.23	78.31	17.95
December	4.79	5.71	4.55	0.93	0.24	79.59	18.95
Mean	**4.24**	**5.20**	**4.03**	**0.96**	**0.21**	**77.50**	**16.78**

Table 10 Capacity-factor of PV arraydeployed at different locations

Location	Solar rating (kWp)	Capacity factor (%)	Reference
Crete	171.4	15.26	Kymakis et al. (2009)
Dublin, Ireland	1.72	10.10	Ayompe et al. (2011)
Khatkar Kalan	190	9.27	Sharma & Chandel (2013)
Tangier, Morocco	0.250	14.84	Attari et al. (2016)
Lakshadweep	10	16.09	Bhakta & Mukherjee (2016)
Andaman and Nicobar	10	14.61	Kumar et al. (2020)
Krishnanagar	**12.4**	**16.78**	**Present Study**

performance metrics, including yield results, losses, PR, and CF is tabulated in Table 9 is for the designated location's PV system. The annual mean reference, array and final yields for the site are observed as 5.20 h/d, 4.24 h/d, and 4.03 h/d, respectively, with peak yields reached during March and minimum values obtained in July. The yearly average system and array capture loss are 0.21 h/d and 0.96 h/d, respectively, with the highest array capture loss in April (1.26 h/d) and the lowest in July (0.73 h/d). Similarly, March records the highest system loss (0.25 h/d), while July exhibits the lowest (0.16 h/d). Furthermore, the CF and PR at the proposed site are 16.78% and 77.50%, respectively. Thus, the performance metrics obtained for this site align with the directives issued by the IEC standard 61724 (CODE & P., 1998), making it suitable for solar PV deployment.

To further validate the deployment of the solar energy system at the proposed site, performance indices obtained in present study are compared with those documented by researchers worldwide. The parameters such as PR and CF provide insights into the efficiency of solar energy conversion to electrical energy. Table 10 presents CF values for PV arrays deployed in different locations. The results indicate significantly higher CF values for tropical regions compared to temperate and Mediterranean regions. Notably, the CF

obtained in the present study surpasses those deployed in locations such as Khatkar-Kalan (Sharma & Chandel, 2013), Dublin (Ayompe et al., 2011), Tangier (Attari et al., 2016), Andaman and Nicobar (Kumar et al., 2020), Crete (Kymakis et al., 2009), and Lakshadweep (Bhakta & Mukherjee, 2016).

Similarly, the PR of PV arrays tends to be higher in tropical and sub-tropical regions, as illustrated in Fig. 10. The present study reveals a PR superior to those observed in Andaman and Nicobar Island (64.93%), Lakshadweep (65.83%), Crete (67.36%), and Khatkar-Kalan (74%). Consequently, a comprehensive comparative assessment of performance indices across different locations strongly supports the utilization of solar energy at the designated site. This underscores its potential for maximizing solar energy efficiency, particularly in light of prevailing sunny conditions.

7.2 Techno-economic analysis

Based on the load estimation of the considered location and the cost of components utilized in the IPGS, simulation results have been obtained from HOMER Pro software. It provides the feasibility of different system architectures. The load estimation and cost breakdown for different components are depicted in Table 2 and Table 7, respectively. The feasible solutions obtained for the considered site include DG only, PV-DG-BCS, DG-BESS-BCS, PV-BESS-BCS and PV-DG-BESS-BCS. These architectures show that a 6.3 kW DG is used along with different sizes of solar PV, converter, and battery to determine various system configurations.

A comprehensive analysis of various feasible system architectures based on technical parameters such as system cost, sizing, RF and fuel consumed is presented in Table 11. The analysis reveals that the initial investment for DG only, PV-DG-BCS, DG-BESS-BCS, PV-BESS-BCS, and PV-DG-BESS-BCS setups are $3150, $24,634.90, $8053.75, $30,619.25 and $23,763.08 respectively. It is evident that PV-BESS-BCS configuration demands the highest capital investment due to requirement of higher battery rating, while the DG only configuration necessitates the lowest investment owing to its use of only single components. Further, it is found that the annual operating cost for DG only, PV-DG-BCS, DG-BESS-BCS, PV-BESS-BCS, and PV-DG-BESS-BCSPV-DG-BCS, DG-BESS-BCS, PV-BESS-BCS, and PV-DG-BESS-BCS configurations are $11,454.22, $8605.09, $6712.31, $712.15, and $917.79 respectively. It has been noted that the PV-BESS-BCS configuration

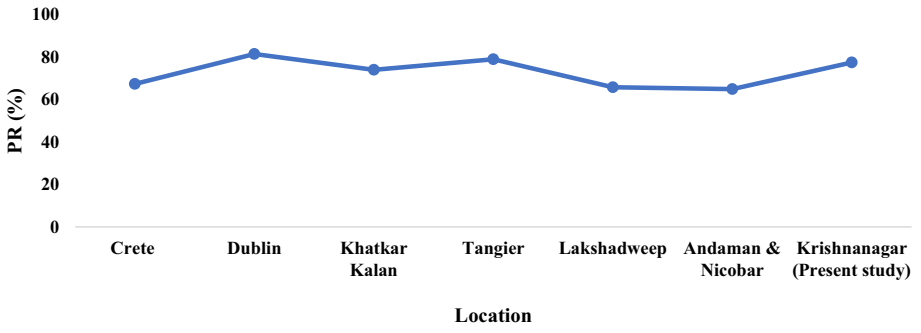

Fig. 10 Performance-ratio of Solar PV array installed at various locations (Attari et al., 2016; Ayompe et al., 2011; Bhakta & Mukherjee, 2016; Kumar et al., 2020; Kymakis et al., 2009; Sharma & Chandel, 2013)

Table 11 Optimal solution in the context of renewable fraction, sizing and cost

Architecture	Solar PV rating (kW)	DG rating (kW)	Battery (kWh)	Converter rating(kW)	Operating cost (in $/yr)	Initial cost ($)	RF (%)	DG fuel (L/yr)
PV-DG-BESS-BCS	12.40	6.30	19.00	4.83	917.79	23,763.08	96.66	165.84
PV-BESS-BCS	15.61		36.00	5.68	712.15	30,619.25	100	0.00
DG-BESS-BCS		6.30	6.00	3.05	6712.31	8053.75	0.00	4176.33
PV-DG-BCS	26.48	6.30		2.86	8605.09	24,634.90	0.00	4908.15
DG only		6.30			11,454.22	3150.00	0.00	6711.84

has the lowest operating cost whereas the DG only setup has the highest. This disparity underscores the pivotal role of DG in meeting load demands, directly impacting its fuel consumption and consequent operating expenses. For instance, the DG-only configuration consumes a substantial 6711 L per year, significantly inflating operating costs. Conversely, the absence of DG in the PV-BESS-BCS architecture results in lowest operating costs. Thus, it is evident that incorporating a PV array greatly reduces the system's operating cost, thereby enhancing its economic viability.

Further, regarding sizing, it is noteworthy that the PV size is smallest in the PV-DG-BESS-BCS configuration (12.4 kW) relative to other setups, while the DG size remains constant at 6.30 kW across different configurations. The solar PV size is notably larger than that of the DG, resulting in various feasible system configurations. This discrepancy arises from HOMER's algorithm, which prioritizes configurations based on NPC and COE. Lower capacity DG requires relatively less fuel, leading to decrease NPC and COE and, consequently, a smaller DG size. Additionally, the findings reveal that there is a significant reduction in fuel consumption for the PV-DG-BESS-BCS configuration. This is attributed to the substantial portion of energy generated by solar PV, with only a minor share generated through DG, signifying minimal fuel usage by this topology. Consequently, the system exhibits a very high RF of 96.66%.

Furthermore, for determining the feasibility of different system configurations, the NPC and COE for each viable option fulfilling the energy requirements of the considered site are being analysed. The COE and NPC values of viable configurations are shown in Table 12. For the DG only, PV-DG-BCS, DG-BESS-BCS, PV-BESS-BCS, and PV-DG-BESS-BCS setups, the NPC and COE are reported as ($151,224.60 & 1.055 $/kWh), ($135,877.30 & 0.948 $/kWh), ($94,827.21 & 0.661 $/kWh), ($39,825.63 & 0.278 $/kWh), and ($35,627.85 & 0.248 $/kWh) respectively. The PV-DG-BESS-BCS arrangement demonstrates the minimum NPC and COE, while the DG only set up provides the highest values. Specifically, for the PV-DG-BESS-BCS set up, NPC is $35,627.85, and COE is 0.248 $/kWh. Thus, based on the above findings, it is evident that the optimal system architecture, comprising 12.4 kW of solar PV, 6.3 kW of DG, 4.83 kW of BCS, and 19 kWh of BESS, demonstrates superior performance in context of NPC, COE, RF and fuel consumption. This optimal configuration is discussed in detail in the preceding sections.

7.3 Performance analysis of optimal IPGS

The optimal system architecture of IPGS comprising 12.4 kW of solar PV, 6.30 kW of DG, 19 numbers of batteries of 1 kWh each and 4.83 kW of converter for delivering a load demand of 30.39 kWh/day at the considered location. The COE and NPC of the

Table 12 Optimization results of various configurations in terms of NPC and COE

Architecture	NPC ($)	COE ($/kWh)
PV-DG-BESS-BCS	35,627.85	0.248
PV-BESS-BCS	39,825.63	0.278
DG-BESS-BCS	94,827.21	0.661
PV-DG-BCS	135,877.30	0.948
DG only	151,224.60	1.054

Table 13 Cost break-up of components of PV-DG-BESS-BCS configuration (Lilienthal, 2016a, 2016b)

Components	Capital investment ($)	Replacement cost ($)	O&M ($)	Fuel rate ($)	Salvage value ($)
DG	3150.00	0.00	544.86	2572.73	474.14
PV	8955.19	0.00	1596.80	0.00	0.00
BESS	7790.00	5755.14	2456.23	0.00	899.36
BCS	3867.89	0.00	312.51	0.00	0.00
System	23,763.08	5755.14	4910.40	2572.73	1373.50

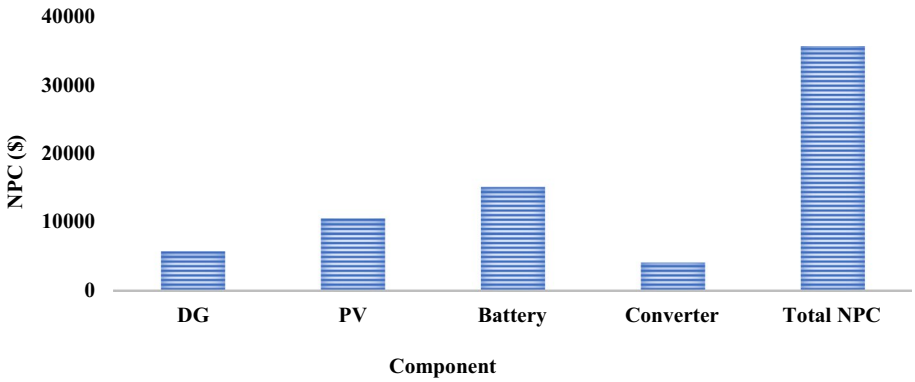

Fig. 11 NPC based on components of IPGS (Lilienthal, 2016a, 2016b)

configuration are 0.248 $/kWh and $35,627.85, respectively, with annual fuel consumption of 165.84 L and a RF of 96.66%

In the proposed IPGS, initial capital investment required for the project amount to $23,763.08, constituting approximately 66% of the overall NPC of the system. Out of which, solar PV and BESS shares significant portion of capital investment with about 69% of system's total NPC. Further, it is found that among all the components, only battery needs to be replaced, which costs $5755.14. Additionally, overall O&M expenses of the system is obtained as $4910, with the battery accounting for 50% of this amount, due to its higher maintenance requirements. The converter, characterized by the absence of moving parts and the rapid advancements of semi-conductor switches requires least maintenance. The fuel price is only about 7% of total NPC, indicating minimal usage of fuel by the proposed IPGS. Correspondingly, salvage value, is about 3% of the total NPC, indicating retained amount within the system and it is denoted as negative value which does not infer actual cost. The cost summary of the proposed configuration based on NPC-cost type is illustrated in Table 13

Moreover, NPC of different components, such as DG, PV, BESS, and BCS, is obtained as $5793.45, $10,551.99, $15,102.01 and $4180.4, respectively for the proposed IPGS. Figure 11 shows the cost summary of the proposed IPGS for the selected site based on component type. It is observed that among all the components, the BESS possesses highest NPC value of $15,102.01, which is about 42% of total NPC of the system, attributed to its higher replacement and O&M expenses. In contrast, the BCS exhibits the lowest NPC value of $4180.4, which is evident from its lower maintenance cost during project's life

time. Further, the solar PV system possess about 30% of total NPC of the system, which is second most after battery due to its higher initial capital investment.

The solar resource is the only renewable source considered in the proposed IPGS. Table 3 shows various technical specifications such as derating factor, efficiency, temperature co-efficient, NOCT etc., of the PV array considered for this study. The temperature co-efficient and NOCT of solar PV are -39/°C and 45 °C, respectively. The average output of the PV array for the selected region is obtained as 52.5 kWh. Figure 12 depicts the PV array output for the selected site. The graph reveals distinct patterns in daily energy production by solar PV. The maximum solar PV output is typically observed between 11:00 AM and 2:00 PM due to the presence of high levels of solar irradiance, with an average output during that period of about 5.34 kW. Correspondingly, lower solar PV output is obtained during the remaining time of the day, with an average output of 2.76 kW. Correspondingly, lower solar PV output is obtained during remaining time of the day with an average output of 2.76 kW. Furthermore, it is observed that solar PV exclusively generates power during the daylight hour (06:00–18:00) with a mean value of 2.19 kW and during the remaining period, solar PV output is zero. Additionally, seasonal influences are apparent from the figure, with the monsoon season (June–September) leading to decreased output due to cloudy atmospheric conditions. Conversely, increased solar PV production is observed during the summer (March–May) and winter (November to February) seasons, attributed to a higher CI of the atmosphere. Moreover, the total production by the PV array for the proposed site is estimated as 19,166 kWh/yr. Other specifications of the PV array, such as rated capacity, capacityfactor, hours of operation, solar penetration and levelized cost, are 12.4 kW, 17.7%, 4391 h/yr, 173% and 0.0426 $/kWh, respectively.

The primary purpose of the DG used in the proposed Integrated Power Generation System (IPGS) is to enhance system reliability. The generator rating for the IPGS is 6.3 kW, with an annual fuel consumption of 165.84 L. This results in an average fuel consumption of 0.454 L per day and 0.0189 L per hour. Additionally, it is found that 0.448 L of diesel is consumed by the generator to produce 1 kWh of energy. The total annual emissions for CO, CO_2, unburned HC, PM, SO_2, and NO_x amount to 2.74 kg, 434 kg, 0.119 kg, 0.0166 kg, 1.06 kg, and 2.57 kg, respectively. The study indicates a significant reduction in the emission of toxic gases with the proposed configuration. Figure 13 shows the DG power output considered in IPGS. The average electrical output for the DG is 1.66 kW, with maximum and minimum output of 4.01 kW and 1.58 kW,

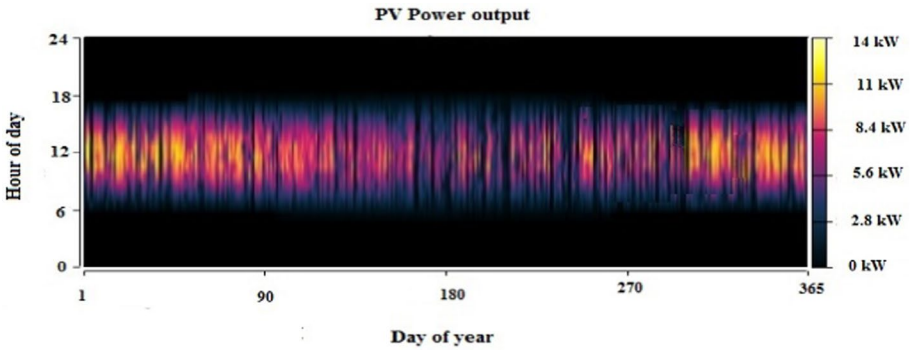

Fig. 12 Solar PV array output for PV-DG-BESS-BCS configuration

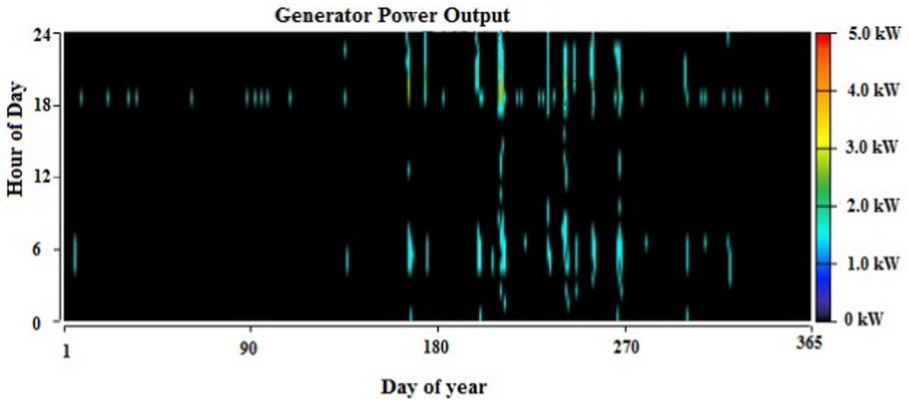

Fig. 13 DG power output for PV-DG-BESS-BCS configuration

respectively. Furthermore, it is observed that DG operation in the proposed configuration is relatively high during the monsoon months (June–September) due to insufficient solar irradiance. Most of the DG power output is obtained during non-daylight hours when the solar PV system is inactive. With an annual fuel energy input of approximately 1630 kWh, the DG system produces 370 kWh of energy in the proposed configuration, resulting in an efficiency of 22.7%. The capacity factor of the DG setup in the IPGS configuration is found to be 0.67%. Additionally, the DG starts 97 times per year in the proposed configuration, indicating limited operation in the design. The DG operates for around 223 h annually, with an estimated operational life of around 80 years.

The power converter is a pivotal and central element in the design of IPGS, enabling the transformation between DC and AC power. With a capacity of 4.83 kW, the converter has a mean output of 1.23 kW and a maximum output of 4.39 kW. Furthermore, it has been determined that for an annual electrical energy input of 11,423.6 kWh, the converter yields an annual electrical output of 10852.3 kWh, resulting in an annual converter loss of 571.33 kWh. Additionally, converters in this system operate for approximately 8750 h per year.

Another vital component considered in this optimal configuration is BESS. The battery stores energy when electrical production exceeds the demand and delivers energy when the production is less than the demand. The specifications of the BESS utilized for this study are presented in Table 4. The nominal voltage, maximum charge current, and battery capacity rating of BESS used in IPGS design are 12 V, 43A, and 260 Ah, respectively. For this optimal configuration, 19 batteries of 1 kWh each with the specifications mentioned aforesaid are used. Figure 14 and Fig. 15 show the monthly and yearly SOC profile of BESS. It is obtained that the yearly average SOC of the battery is about 67.63%for the proposed IPGS. The annual average SOC of the battery indicates its capability to store 5710kWh/yr of energy and effectively meet the system's energy requirements. Additionally, a decrease in SOC is observed during the monsoon months, averaging 59.3%. This decline aligns with the reduced sunlight exposure and subsequent decrease in solar PV output during this period, affecting the energy input to the battery. Moreover, the losses incurred in battery energy storage are found to be1486 kWh/yr with an annual storage depletion of 21.8kWh. The BESS also demonstrates impressive longevity, with a lifetime throughput of approximately 68,050 kWh, translating to an annual throughput of 6629 kWh/yr.

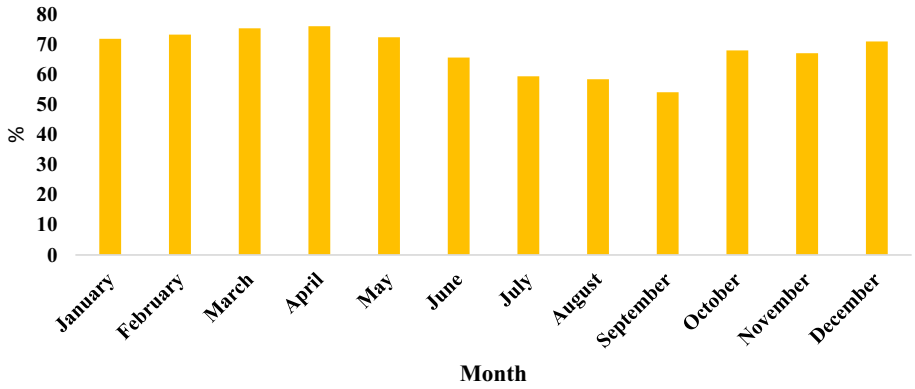

Fig. 14 Monthly SOC profile of BESS for PV-DG-BESS-BCS configuration

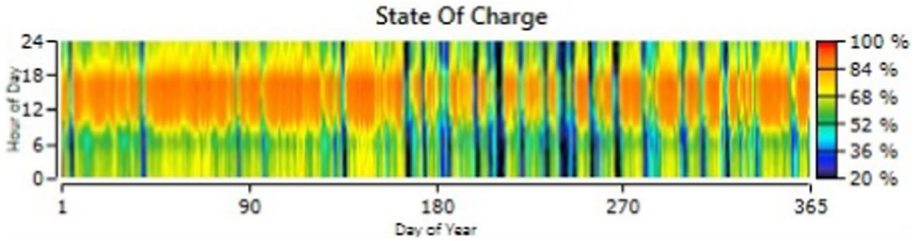

Fig. 15 Yearly SOC profile of BESS for PV-DG-BESS-BCS configuration

The proposed IPGS yields a total electrical energy output of 19,536 kWh per year, while the energy consumption for the specified location is 11,092 kWh per year. This results in an annual excess energy production of 6414 kWh, with the remaining 2030 kWh/year contributing to losses incurred by the converter and the battery. It is noteworthy that the majority of total electrical energy production, approximately 98.1%, is attributed to solar PV, with the remaining 1.89% generated by the DG.

In order to further validate the proposed configuration, a 24-h time series analysis was examined, depicting the hourly operation of various components in the proposed IPGS for a typical day (1st of May), as shown in Fig. 16. The figure highlights the following key points:

- During (00:00–06:00) hour: Energy demand is minimum, approximately 0.25 kW. Energy generated by solar PV is zero due to the lack of solar radiation. Battery discharges to meet the energy requirement.
- During (06:00–18:00): Average load served during the period is about 1.55 kW. Solar PV starts generating power due to the presence of solar energy. Energy generated by PV array is about 3.90 kW. Energy generated exceeds the load demand. BESS stores excess energy.
- During (18:00–23:00)-Energy demand reaches its peak (3.76 kW). Solar PV does not produce power due to unavailability of solar energy. Battery discharges to meet the load demand.

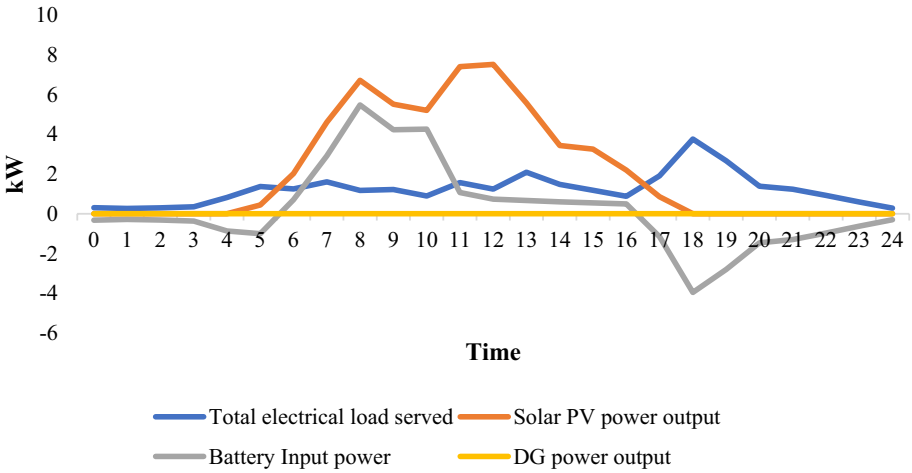

Fig. 16 Power flow of various components involved in PV-DG-BESS-BCS configuration for a single day (1st of May

Thus, it is observed that during the daytime, solar PV generation surpasses the demand. This surplus energy is stored in the battery during daylight hours. As power produced by PV is more than enough to satisfy load demand, so DG used in this IPGS system does not require to operate for power generation. However, because of the unavailability of solar radiation at night, PV array ceases energy generation. As such, the battery discharges to meet the energy requirement at night. Therefore, high renewable fraction of the system is observed at the considered location.

7.4 Sensitivity analysis

To further consolidate the motive for using the proposed configuration at the considered location, sensitivity analysis is being conducted. The system is subjected to analyze by defining and varying various sensitivity variables. These sensitivity variables are selected to demonstrate their effect on power generation and their influence on the system economics.

In the proposed configuration of IPGS, there are two sources of energy solar PV and DG. The DC power of PV array greatly depends on its derating factor. It signifies the losses incurred in the solar PV array due to factors such as shading, dust accumulation, and wiring losses. Besides, ambient temperature significantly influences solar PV generation. Furthermore, the amount of fuel consumed and the price of diesel greatly impact the system's economics. Thus, derating factor, ambient temperature and diesel fuel price are selected as the sensitivity variables for the proposed work.

To conduct sensitivity analysis for the proposed IPGS at the considered location these factors are varied non-linearly over a wide range to see the system response and its effect on the performance parameters like NPC, COE and RF. The derating factor varied non-linearly over a range of (79%-99%). Simultaneously, diesel fuel prices are varied over a wide range, spanning from (0.7 $/L-1.27 $/L). Subsequently, the ambient temperature is maintained at 26.04 °C, 28 °C and 30 °C. Thus, for the same resources and load conditions

of the specified location, these selected variables are varied together within the above-mentioned range.

In the present study, a derating factor of 88%, an ambient temperature of 26.04 °C and a diesel fuel price of $1.2/L are considered as the basis of analysis. When the derating factor is nonlinearly decreased from its operational value, the NPC and COE increases with a decrease in RF. Conversely, a nonlinear increase in the derating factor from its operational value leads to a reduction in the NPC and COE of the system as the RF increases. Additionally, a decrease in diesel fuel rate leads to reduction in the values of NPC and COE, and vice versa. Furthermore, the increased in ambient temperature of the selected region results in increased value of NPC and COE with decrease in RF. The detailed influence of these selected variables on various parameters such as RF, NPC and COE is tabulated in Table 14.

Additionally, as the derating factor is increased while keeping other parameters constant, there is a decrease in NPC and COE as the system's RF increases. Likewise, with an increase in diesel fuel price while maintaining a constant derating factor and ambient temperature, there is a corresponding increase in both COE and NPC of the system. Similarly, with an increase in the average ambient temperature of the selected site, both COE and NPC of the system increase, while RF decreases, assuming the other two sensitivity variables remain at a fixed value.

Moreover, it is found that if the PV array's derating factor is kept constant and there is a simultaneous rise in average ambient temperature and diesel fuel rate, the COE and NPC of the system increases. Further, with the simultaneous hike in derating factor of solar PV and diesel fuel rate, keeping the average ambient temperature constant decreases the values of COE and NPC. Similarly, with no variation in the diesel fuel rate, if the remaining two sensitivity variables are raised simultaneously, the COE and NPC values get reduced.

In order to get a proper insight into sensitivity analysis for the proposed configuration, consider the surface plot between sensitivity variables with COE superimposed on NPC, as shown in Fig. 17. It depicts that for the proposed configuration, NPC and COE possess the least value for derating factor of 99% and diesel fuel rate of $0.7 per litre. This figure also shows that with the increase in the price of diesel fuel price and the decrease in the PV array's derating factor, the COE and NPC values get increased. Moreover, Fig. 18 shows an optimization plot between COE and the RF of the system. Each point on the optimization plot is a viable solution. The plot is obtained by varying COE and RF keeping derating factor at 88%. The figure depicts that as the RF of the system increases COE of the system reduces. It is worth noting that the COE of the system increases when shifting from a hybrid to a diesel energy system and decreases when reverting back to a hybrid system. Thus, putting the system subjected to sensitivity analysis further validates the point of using the proposed configuration for the selected site.

7.5 Statistical Analysis for validation

The statistical significance for the evaluated results is carried out using linear regression method. The average solar PV power output (E_{DC} and E_{AC}) obtained during the analysis are compared with their predicted values. The percentage differences in the values of DC and AC energy output reveal a narrow range between the obtained and predicted values. Figure 19 shows the percentage difference values for both parameters, with the percentage variance in DC energy values, ranging from -2.68% to 2.78%

Table 14 Sensitivity response of PV-DG-BESS-BCS configuration at the considered location (Lilienthal, 2016a, 2016b; Multiple data access option, National Aeronautics & Space Administration, 2021)

Sensitivity variables			System parameters		
Derating factor (%)	Diesel fuel price ($/L)	Ambient temperature (°C)	NPC ($)	COE ($/kWh)	Renewable fraction (%)
79	0.7	26.04	35,191.24	0.244	92.53
79	0.7	28.04	35,250.87	0.245	92.57
79	0.7	30.04	35,345.84	0.246	92.54
84	0.7	26.04	34,593.55	0.240	92.62
84	0.7	28.04	34,659.51	0.241	92.62
84	0.7	30.04	34,754.00	0.242	92.56
88	0.7	26.04	34,151.80	0.237	92.78
88	0.7	28.04	34,248.08	0.238	93.74
88	0.7	30.04	34,269.78	0.238	92.57
94	0.7	26.04	33,520.17	0.233	93.40
94	0.7	28.04	33,607.55	0.233	94.11
94	0.7	30.04	33,680.21	0.234	93.42
97	0.7	26.04	33,237.48	0.231	94.56
97	0.7	28.04	33,317.40	0.231	94.30
97	0.7	30.04	33,388.51	0.232	93.74
99	0.7	26.04	33,062.90	0.230	94.61
99	0.7	28.04	33,116.21	0.231	94.79
99	0.7	30.04	33,210.15	0.231	93.82
79	1.1	26.04	36,547.08	0.254	95.88
79	1.1	28.04	36,635.20	0.255	95.60
79	1.1	30.04	36,740.44	0.255	95.79
84	1.1	26.04	35,879.39	0.249	95.96
84	1.1	28.04	35,997.19	0.250	95.75
84	1.1	30.04	36,076.24	0.251	95.81
88	1.1	26.04	35,408.49	0.246	96.63
88	1.1	28.04	35,495.70	0.247	95.80
88	1.1	30.04	35,599.65	0.247	95.83
94	1.1	26.04	34,731.95	0.241	96.43
94	1.1	28.04	34,829.59	0.242	95.92
94	1.1	30.04	34,925.61	0.243	95.88
97	1.1	26.04	34,454.54	0.239	96.61
97	1.1	28.04	34,528.15	0.240	96.15
97	1.1	30.04	34,597.51	0.240	96.20
99	1.1	26.04	34,243.44	0.238	96.63
99	1.1	28.04	34,332.10	0.238	97.23
99	1.1	30.04	34,412.05	0.239	96.42
79	1.2	26.04	36,816.36	0.256	95.92
79	1.2	28.04	36,900.62	0.256	95.88
79	1.2	30.04	36,989.79	0.257	95.84
84	1.2	26.04	36,123.23	0.251	96.09
84	1.2	28.04	36,236.50	0.252	95.97
84	1.2	30.04	36,334.24	0.252	96.11

Table 14 (continued)

Sensitivity variables			System parameters		
Derating factor (%)	Diesel fuel price ($/L)	Ambient temperature (°C)	NPC ($)	COE ($/kWh)	Renewable fraction (%)
88	1.2	26.04	35,627.50	0.248	96.67
88	1.2	28.04	35,764.50	0.249	96.04
88	1.2	30.04	35,844.40	0.250	96.12
94	1.2	26.04	34,988.25	0.244	96.78
94	1.2	28.04	35,073.67	0.245	96.11
94	1.2	30.04	35,205.70	0.245	96.17
97	1.2	26.04	34,669.39	0.241	96.82
97	1.2	28.04	34,767.48	0.242	96.34
97	1.2	30.04	34,845.98	0.242	96.22
99	1.2	26.04	34,480.19	0.240	96.93
99	1.2	28.04	34,580.62	0.242	96.78
99	1.2	30.04	34,640.13	0.242	96.33
79	1.25	26.04	36,955.26	0.257	95.59
79	1.25	28.04	37,044.83	0.258	95.62
79	1.25	30.04	37,150.02	0.258	96.05
84	1.25	26.04	36,247.00	0.252	96.09
84	1.25	28.04	36,360.12	0.253	95.87
84	1.25	30.04	36,449.66	0.253	96.09
88	1.25	26.04	35,770.40	0.249	96.22
88	1.25	28.04	35,852.70	0.250	96.09
88	1.25	30.04	35,943.50	0.251	96.41
94	1.25	26.04	35,083.40	0.245	96.30
94	1.25	28.04	35,165.84	0.246	96.36
94	1.25	30.04	35,249.74	0.245	96.43
97	1.25	26.04	34,809.79	0.243	96.39
97	1.25	28.04	34,885.77	0.243	96.50
97	1.25	30.04	34,945.39	0.243	96.48
99	1.25	26.04	34,578.92	0.241	96.66
99	1.25	28.04	34,669.61	0.242	96.57
99	1.25	30.04	34,752.81	0.243	96.61
79	1.27	26.04	37,019.93	0.258	96.27
79	1.27	28.04	37,108.99	0.258	96.41
79	1.27	30.04	37,211.30	0.259	96.23
84	1.27	26.04	36,307.52	0.253	96.43
84	1.27	28.04	36,420.99	0.254	96.45
84	1.27	30.04	36,514.89	0.254	96.26
88	1.27	26.04	35,845.09	0.250	96.47
88	1.27	28.04	35,932.24	0.251	96.55
88	1.27	30.04	36,026.82	0.251	96.73
94	1.27	26.04	35,155.62	0.244	96.49
94	1.27	28.04	35,244.54	0.246	96.60
94	1.27	30.04	35,336.13	0.246	96.75

Table 14 (continued)

Sensitivity variables			System parameters		
Derating factor (%)	Diesel fuel price ($/L)	Ambient temperature (°C)	NPC ($)	COE ($/kWh)	Renewable fraction (%)
97	1.27	26.04	34,875.75	0.242	96.60
97	1.27	28.04	34,945.86	0.244	96.62
97	1.27	30.04	35,028.71	0.244	96.79
99	1.27	26.04	34,671.66	0.242	96.64
99	1.27	28.04	34,732.61	0.243	96.65
99	1.27	30.04	34,864.47	0.243	96.80
79	1	26.04	36,332.76	0.253	95.49
79	1	28.04	36,418.22	0.253	95.31
79	1	30.04	36,512.70	0.254	95.56
84	1	26.04	35,677.94	0.248	95.67
84	1	28.04	35,765.70	0.249	95.79
84	1	30.04	35,848.53	0.249	96.03
88	1	26.04	35,193.59	0.244	96.15
88	1	28.04	35,293.81	0.245	96.11
88	1	30.04	35,358.30	0.246	96.18
94	1	26.04	34,548.52	0.240	96.17
94	1	28.04	34,641.96	0.240	96.16
94	1	30.04	34,706.63	0.240	96.25
97	1	26.04	34,239.95	0.237	96.18
97	1	28.04	34,307.62	0.238	96.23
97	1	30.04	34,416.37	0.238	96.31
99	1	26.04	34,054.70	0.235	96.29
99	1	28.04	34,122.47	0.236	96.32
99	1	30.04	34,237.20	0.237	96.85

and that of AC energy lying in the range of -2.25% to -3.38%. The graph demonstrates minimal disparity between the obtained and predicted values, underscoring the credibility of the results.

Further, the degree of accuracy for the performance indices obtained in the analysis are examined by using various statistical metrics like mean-percentage error (MPE), mean-bias error (MBE), and root-mean-square error (RMSE). Further, MBE offers insights into the system's long-term performance, while RMSE evaluates short-term performance. A lower value indicates greater accuracy, and a positive MBE suggests overestimation, whereas a negative value signifies underestimation by the system (Tarhan & Sarı, 2005). In addition to these parameters, the proposed study incorporates mean percentage error to ascertain the statistical significance of the obtained results (Yao et al., 2014).

To evaluate the statistical significance of the results, a comparison is made by analysing the best fit regression values for different performance metrics of the PV array.Table 15presents the statistical indicators for various performance indices at the considered location. The more closely the value of the regression coefficient (R^2) aligns with unity, the greater the accuracy of the system. The regression co-efficient for final yield, array yield, reference yield PR and CF of the solar PV array are observed to be close to unity, with values

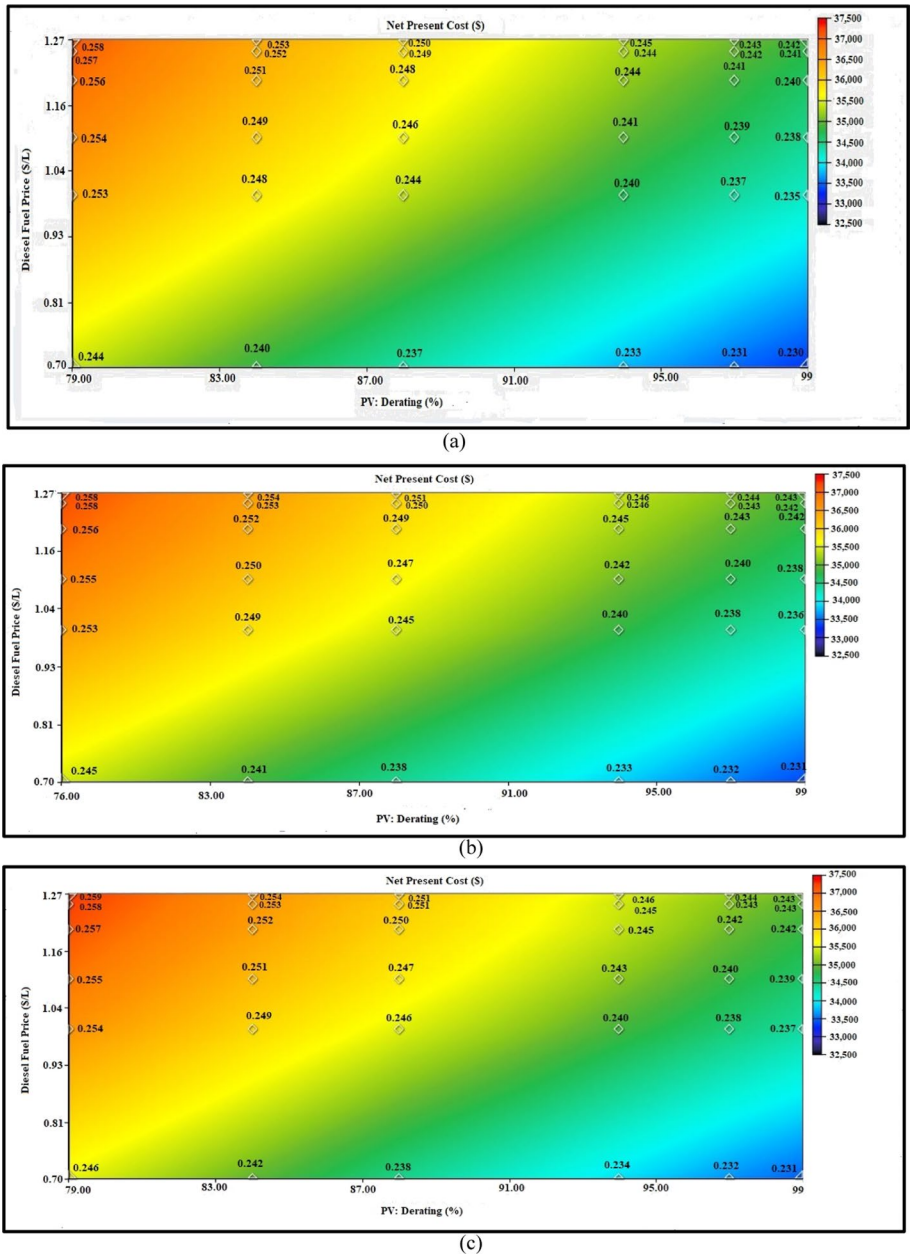

Fig. 17 Graph showing COE superimposed on NPC for PV-DG-BESS-BCS configuration for the considered location at temperature (a) 26.04 °C (b) 28.04 °C (c) 30.04 °C

of 0.977, 0.971, 0.987, 0.919, and 0.945, respectively. Correspondingly, RMSE, MBE and MPE are evaluated using Eqs. (9–11) (Sundaram & Babu, 2015). Thus, obtained results in terms of performance of PV array at the considered location are statistically significant.

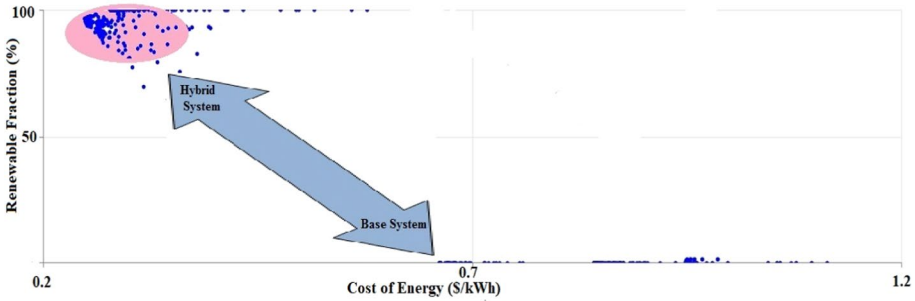

Fig. 18 Optimization plot of PV-DG-BESS-BCS configuration based on COE and Renewable fraction

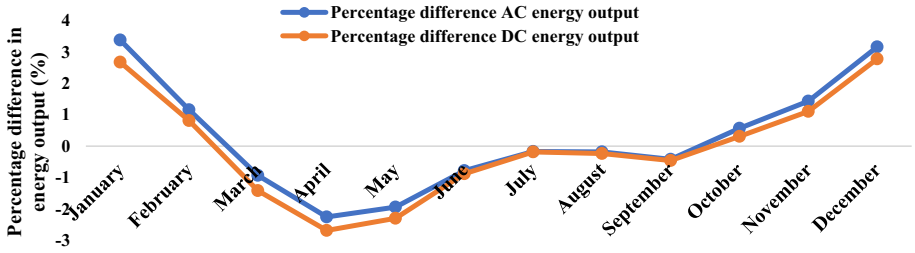

Fig. 19 Percentage difference in energy output

Table 15 Statistical metrics for performance indices of PV array

Performance metrics	MBE	MPE (%)	RMSE	R^2
$Y_{reference}$	0.0036	0.27	0.04	0.987
Y_{array}	0.0288	0.43	0.046	0.971
Y_{final}	0.0092	0.21	0.038	0.977
PR	0.1123	0.13	0.204	0.919
CF	0.1217	0.72	0.234	0.945

$$MBE = \left(\frac{1}{N}\right)\sum_{i=1}^{k}\left[(predicted) - (obtained)\right] \tag{9}$$

$$MPE = \left(\frac{1}{N}\right)\sum_{i=1}^{k}\left[\frac{\{(predicted) - (obtained)\}}{(obtained)}\right]X100 \tag{10}$$

$$RMSE = \sqrt{\frac{1}{N}\sum_{i=1}^{k}\left[(predicted) - (obtained)\right]^2} \tag{11}$$

Moreover, the interdependence of the output performance parameter E_{DC} on input variables such as ambient temperature, solar radiation, and PV cell temperature is explored

using the best fit regression coefficient (R^2). Three separate analyses have been conducted to assess R^2. The first analysis involves E_{DC} and solar radiation, the second focuses on E_{DC} and ambient temperature, and the third examines E_{DC} and PV cell temperature. The best fit regression coefficient for E_{DC} and solar radiation is found to be close to unity, with a value of 0.985. In contrast, the corresponding values of R^2 for the second and third cases are 0.164 and 0.058, respectively This suggests that the variation in solar PV power output is predominantly influenced by changes in solar radiation at the considered location. Figure 20 shows the plot between E_{DC} and solar radiation, showing best fit regression coefficient of 0.985. Thus, thorough statistical analysis affirms the robustness and statistical significance of the obtained results, enhancing the study's credibility and underscoring the suitability of deploying a PV array at the considered site.

8 Comparative Analysis

This section provides comparative analysis between the proposed configuration and a base system based on economics and emissions. The main motive of this analysis is to demonstrate the superiority of the proposed configuration over the base system for the designated site. The proposed system comprises solar PV, DG, battery, and converter with sizes of 12.4 kW, 6.3 kW, 19 kWh, and 4.83 kW, respectively. In contrast, the base system is a DG-only configuration with a size of 6.3 kW.

Table 16 presents a comparative analysis based on economics for both the base and proposed configurations. The results indicate a significant reduction of 76.4% in the values of NPC and COE when the proposed IPGS configuration is employed instead of the base system at the designated location. Additionally, the operating cost for the proposed IPGS configuration is notably lower compared to that of the base system. Specifically, the operating costs for the proposed IPGS configuration and the base system are $917.79 and $11,454.22, respectively.

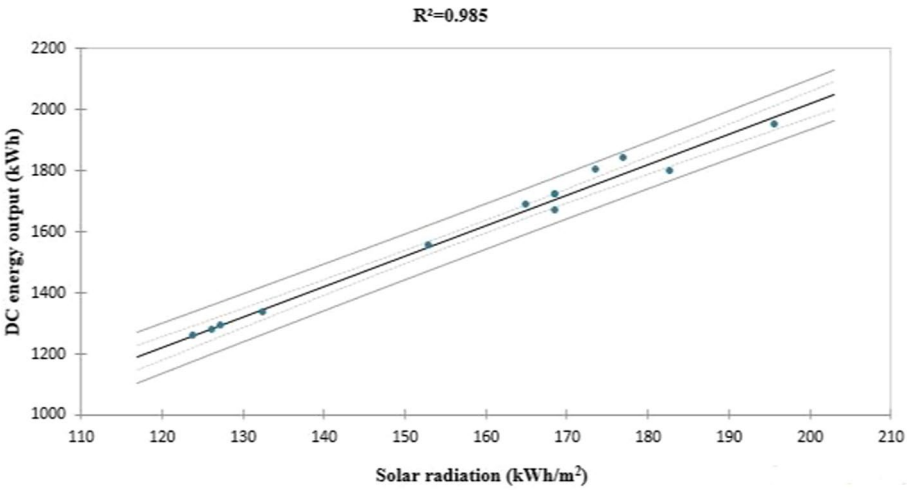

Fig. 20 Graph showing regression plot between E_{DC} and Solar radiation

Table 16 Comparison based on economics proposed IPGS with the base case

Parameters	DG only	PV-DG-BESS-BCS
Initial-cost ($)	3150	23763.08
Operating-cost ($/yr)	11454.22	917.79
NPC ($)	151224.60	35627.85
COE ($/kWh)	1.054	0.248

In the context of harmful gas emissions, the proposed configuration shows splendid results compared to the base system. The annual CO_2 emission from the proposed configuration is only about 2.5% of those from the base system. Table 17 summarizes the emission of pollutants for both the configurations. It's evident from the table that the total annual fuel consumption of the base configuration significantly exceeds that of the proposed configuration. For the DG only configuration, the annual emission of pollutants such as CO, CO_2, unburned HC, SO_2, PM, and NO_x configuration are 111 kg, 17,569 kg, 4.83 kg, 43 kg, 0.671 kg, and 104 kg, respectively. In comparison, the proposed configuration results in drastically reduced pollutant emissions, with values of 2.74 kg, 434 kg, 0.119 kg, 1.06 kg, 0.016 kg, and 2.57 kg for CO, CO_2, unburned HC, SO_2, PM and NO_x, respectively.

Additionally, a comparative analysis based on economic parameters (NPC and COE) was conducted comparing against the existing literature to ascertain the economic feasibility of the proposed configuration at the study location. Table 18 illustrates the COE and NPC estimates for the PV-DG-BCS-BESS configuration across various locations. For instance, in Salehin et al. (2016), a load of 218 kWh/d in Kutubdia, Bangladesh, yielded a COE of 0.35 $/kWh and an NPC of $218,615. Similarly, (Das et al., 2017) reported an NPC of $223,457 and a COE of 0.32 $/kWh for a 210 kWh/d load in South Australia. Notably, (Kumar et al., 2021b) revealed NPC and COE values of $47,345.65 and 0.33 $/kWh, respectively, for a daily load of 30.45 kWh in the Minicoy region of India. Moreover, in Odou et al. (2020), the NPC and COE were determined as $555,492 and 0.207 $/kWh, respectively, for a load of 679 kWh/d in Alibori, Benin Republic. Similarly, reference (Pujari & Rudramoorthy, 2021),a COE of 0.217 $/kWh and an NPC of $341,280 for a 332.14 kWh/d load in Andhra Pradesh, India.

Table 17 Comparison of emissions of pollutants of proposed IPGS with the base case

Parameters	DG only	PV-DG-BESS-BCS
Total fuel consumptions (L/year)	6711.83	165.84
Hours of operation (h/year)	8760	223
PM (kg per year)	0.671	0.016
CO (kg per year)	111	2.74
Unburned HC (kg per year)	4.83	0.119
CO_2 (kg per year)	17569	434
Sulphur dioxide (kg per year)	43	1.06
NO_x (kg per year)	104	2.57

Table 18 Comparison of the hybrid stand-alone system at different locations

Location	System Configuration	Load (kWh/d)	NPC ($)	COE ($/kWh)	Reference
Kutubdia, Bangladesh	PV-DG-BCS-BESS	218	218,615	0.35	Salehin et al., 2016)
South Australia	PV-DG-BCS-BESS	210	223,457	0.32	Das et al., 2017)
Minicoy, India	PV-DG-BCS-BESS	30.45	47,345.65	0.33	Kumar et al., 2021b)
Alibori, Benin Republic	PV-DG-BCS-BESS	679	555,492	0.207	Odou et al., 2020)
Andhra Pradesh, India	PV-DG-BCS-BESS	332.14	341,280	0.217	Pujari & Rudramoorthy, 2021)
Krishnanagar, India	PV-DG-BCS-BESS	**30.39**	**35,627.85**	**0.248**	**Present Study**

9 Limitations and implication policies

As the study involves performance assessments of solar PV array and analyzing the effectiveness of solar PV integrated power generation system in a self-sustainable manner, it involves certain limitations. These limitations offer valuable insights into the contextual boundaries and areas for future refinement. Additionally, the study outlines implication policies, providing a roadmap for policymakers and stakeholders to navigate sustainable energy adoption in remote regions. This contributes to a comprehensive understanding of the study and its practical implications. Following are the list of implication policies and limitations of the study.

Limitations

- The study overlooks grid integration in the system design, presuming that excess energy can be absorbed by the grid. This omission fails to address potential challenges related to grid integration.
- The study neglects to account for ohmic losses occurring within the system, which oversights potential inefficiencies in the transmission of energy source and the load, thereby influencing overall performance.

Implication policies

- Regulatory bodies should consider implementing policies that offer financial incentives and subsidies such as tax credits, grants, or favorable financing options for investing in sustainable energy solutions.
- Policymakers should streamline approval processes for obtaining necessary permits and licenses, ensuring a straightforward regulatory pathway for quicker project implementation.
- Stakeholders can attract investments, by introducing feed-in tariffs, providing a fixed, competitive price for the generated electricity can creating a favorable economic environment for off-grid solar projects.
- Policymakers can initiate certification processes to establish quality and safety standards for implemented solar PV systems promoting reliability and longevity in off-grid power generation.

10 Conclusion

This article exclusively investigates the techno-economic viability of solar PV based self-sustained IPGS (PV-DG-BESS-BCS) for supplying uninterrupted, reasonably priced electricity for the considered remote part of eastern India. The proposed study involves assessing solar energy resource at the considered site. In order to analyze solar PV potential, various performance indices are evaluated. The yearly mean final yield, array yield, reference yield, array capture loss and system loss of PV array are calculated to be 4.03 h/d, 4.24 h/d, 5.20 h/d, 0.21 h/d and 0.96 h/d, respectively, with yearly average CF of 16.78% and PR of 77.50%, respectively. The obtained results are as per directives issued by IEC standard 61,724. To further validate the solar potential at the considered location, various performance metrics estimated in the study are statistically validated using regression

analysis. The best-fit regression co-efficient R^2 of these indices indicates the viability of the solar energy resource at the selected site, with values close to unity. Hence, it is concluded that the considered location is highly suitable for the successful implementation solar PV array system.

Moreover, the study reveals that the system configuration consists of 12.4 kW of solar PV, 6.30 kW of DG, 19 kWh of BESS and 4.83 kW of BCS shows the best result for the selected region in terms of minimal COE and NPC, highest RF and lowest carbon emissions. The COE and NPC are obtained to be 0.248 $/kWh and $35,627.85, respectively. Further, it is found that the bulk of electrical energy is produced by solar PV for the proposed configuration as compared to DG, which only shares 1.8% of total electrical energy production. This suggests a very high RF of the system (96.66%), resulting in less fuel consumption, which in turn reduces the emission of harmful gases. The study further reveals that system economics such as COE and NPC get reduced by 76.4% when the proposed configuration is compared to the base system. Also, carbon emission by the proposed configuration is only about 2.5% of the base system. Thus, this research reveals that the proposed design is eco-friendly and offers an affordable price for energy consumption.

Furthermore, to justify the viability of the proposed IPGS, a unique three-dimensional sensitivity analysis is conducted, showing the effect of various uncertain variables such as solar PV derating factor, ambient temperature and diesel fuel rate on system economics and power generation. The study reveals that the increase in the derating factor of solar PV decreases the values of COE and NPC. Likewise, an increase in ambient temperature and diesel fuel rate increases the COE and NPC of the system. Additionally, the study shows that with the increase in RF, COE of the system decreases. This implies that once the system is switched to a hybrid topology, the COE value drops with an increase in the RF of the system.

Therefore, it is concluded that designing a self-sustained renewable energy-based power generating model provides a viable alternative for electrifying remote locations in India. These types of models not only generate clean, sustainable energy but also provide it at a lower cost. Moreover, with the support of the government and the policymakers, the overall investment of the system can get reduced by receiving grants which in turn encourages investors to invest more in similar models and boost the country's economy.

11 Future research and recommendations

In shaping the future trajectory of solar PV based IPGS in energy-deprived regions, there are crucial areas demanding attention for improvement and broader implementation. Firstly, there is a need to enhance efficiency and viability by exploring advanced energy storage technologies, including lithium-ion, lead-acid, and emerging options such as flow batteries or advanced supercapacitors. The investigation of diverse solar tracking systems is imperative to determine the most fitting technology for enhancing the efficiency of integrated solar PV power generation systems. Furthermore, an examination of various PV cell technologies is essential to recognize the most appropriate options for integration into hybrid off-grid power generation systems in remote regions. Efforts should also be directed towards enhancing the adaptability of these systems to diverse geographical contexts, effectively addressing energy crises in various regions. Policymakers hold a pivotal role in facilitating the widespread adoption of sustainable energy solutions through supportive regulations. Moreover, community engagement is paramount, ensuring local communities

actively participate in decision-making and planning processes, fostering widespread acceptance and success. The incorporation of these considerations into future research and implementation will undoubtedly contribute to the continuous development and success of PV systems in remote areas, advancing energy solutions and promoting socio-economic development.

Data availability The data are available from the corresponding author upon request.

References

Abdul-Ganiyu, S., Quansah, D. A., Ramde, E. W., Seidu, R., & Adaramola, M. S. (2021). Techno-economic analysis of solar photovoltaic (PV) and solar photovoltaic thermal (PVT) systems using exergy analysis. *Sustainable Energy Technologies and Assessments, 47*, 101520. https://doi.org/10.1016/j.seta.2021.101520

Adaramola, M. S., & Vågnes, E. E. (2015). Preliminary assessment of a small-scale rooftop PV-grid tied in Norwegian climatic conditions. *Energy Conversion and Management, 90*, 458–465. https://doi.org/10.1016/j.enconman.2014.11.028

Allouhi, A., Saadani, R., Kousksou, T., Saidur, R., Jamil, A., & Rahmoune, M. (2016). Grid-connected PV systems installed on institutional buildings: Technology comparison, energy analysis and economic performance. *Energy and Buildings, 130*, 188–201. https://doi.org/10.1016/j.enbuild.2016.08.054

Ameur, A., Berrada, A., Bouaichi, A., & Loudiyi, K. (2022). Long-term performance and degradation analysis of different PV modules under temperate climate. *Renewable Energy, 188*, 37–51. https://doi.org/10.1016/j.ijhydene.2022.07.088

Attari, K., Elyaakoubi, A., & Asselman, A. (2016). Performance analysis and investigation of a grid-connected photovoltaic installation in Morocco. *Energy Reports, 2*, 261–266.

Awad, H., Nassar, Y. F., Hafez, A., Sherbiny, M. K., & Ali, A. F. (2022). Optimal design and economic feasibility of rooftop photovoltaic energy system for Assuit University. *Egypt. Ain Shams Engineering Journal, 13*(3), 101599. https://doi.org/10.1016/j.asej.2021.09.026

Ayompe, L. M., Duffy, A., McCormack, S. J., & Conlon, M. (2011). Measured performance of a 1 72 kW rooftop grid-connected photovoltaic system in Ireland. *Energy Conversion and Management, 52*(2), 816–825. https://doi.org/10.1016/j.enconman.2010.08.007

Aziz, A. S., Tajuddin, M. F. N., Adzman, M. R., Mohammed, M. F., & Ramli, M. A. (2020). Feasibility analysis of grid-connected and islanded operation of a solar PV microgrid system: A case study of Iraq. *Energy, 19*, 116591. https://doi.org/10.1016/j.energy.2019.116591

Bagheri, M., Delbari, S. H., Pakzadmanesh, M., & Kennedy, C. A. (2019). City-integrated renewable energy design for low-carbon and climate-resilient communities. *Applied Energy, 239*, 1212–1225. https://doi.org/10.1016/j.apenergy.2019.02.031

Bhakta, S., & Mukherjee, V. (2016). Solar potential assessment and photovoltaic generator performance indices analysis for isolated Lakshadweep Island of India. *Sustainable Energy Technologies and Assessments, 17*, 1–10. https://doi.org/10.1016/j.seta.2016.07.002

Bhakta, S., & Mukherjee, V. (2017). Performance indices evaluation and techno economic analysis of photovoltaic power plant for the application of isolated India's island. *Sustainable Energy Technologies and Assessments, 20*, 9–24. https://doi.org/10.1016/j.seta.2017.02.002

Canadian Solar all black CS6K-290MS monocrystalline Canadian Solar module. Canadian Solar Inc. 2019. https://www.canadiansolar.com/wpcontent/uploads/2019/12/InstallationManualofStandardSolarModulesen.pdf/ Accessed 28 Oct 2021

Central electricity authority, executive summary on power sector December 2021<http://www.cea.nic.in/reports/monthly/executivesummary/exe/summary-06.pdf. Accessed 5 Jan 2022.

CODE, P., 1998. Photovoltaic system performance monitoring–Guidelines for measurement, data exchange and analysis.

Das, B. K., Al-Abdeli, Y. M., & Kothapalli, G. (2017). Optimization of stand-alone hybrid energy systems supplemented by combustion-based prime movers. *Applied Energy, 196*, 18–33. https://doi.org/10.1016/j.apenergy.2017.03.119

Das, B. K., & Zaman, F. (2019). Performance analysis of a PV/Diesel hybrid system for a remote area in Bangladesh: Effects of dispatch strategies, batteries, and generator selection. *Energy, 169*, 263–276. https://doi.org/10.1016/j.energy.2018.12.014

Dawoud, S. M., Lin, X. N., Sun, J. W., Okba, M. I., Khalid, M. S., & Waqar, A. (2015). Feasibility study of isolated PV-wind hybrid system in Egypt. *Advanced Materials Research, 1092*, 145–151. https://doi.org/10.4028/www.scientific.net/AMR.1092-1093.145

de Lima, L. C., de Araújo Ferreira, L., & de Lima Morais, F. H. B. (2017). Performance analysis of a grid-connected photovoltaic system in northeastern Brazil. *Energy for Sustainable Development, 37*, 79–85. https://doi.org/10.1016/j.esd.2017.01.004

de Souza Silva, J.L., Costa, T.S., de Melo, K.B., Sakô, E.Y., Moreira, H.S. and Villalva, M.G., 2020, February. A comparative performance of PV power simulation software with an installed PV plant. In *2020 IEEE International Conference on Industrial Technology* (531–535). IEEE. https://doi.org/10.1109/ICIT45562.2020.9067138.

Discover Innovative battery solution. https://discoverbattery.com/assets/dropbox/Datasheets/en/12VRE-3000TF.pdf/. Accessed 1 Nov 2021

District census handbook Nadia series-10 Part XII-a, village and town directory. Census of India; 2011

Duffie, J. A., Beckman, W.A., & Blair, N. (2020). Solar engineering of thermal processes, photovoltaics and wind John Wiley & Sons

Duman, A. C., & Güler, Ö. (2018). Techno-economic analysis of off-grid PV/wind/fuel cell hybrid system combinations with a comparison of regularly and seasonally occupied households. *Sustainable Cities and Society, 42*, 107–126. https://doi.org/10.1016/j.scs.2018.06.029

Esposito, L., Brahmi, M. and Joshi, M., 2023. The Importance of Innovation Diffusion in the Renewable Energy Sector. In *Exploring Business Ecosystems and Innovation Capacity Building in Global Economics* 283–302. IGI Global. https://doi.org/10.4018/978-1-6684-6766-4.ch015

Esposito, L. and Brahmi, M., 2023. Value Creation Through Innovation: Renewable Energy Community. In *Exploring Business Ecosystems and Innovation Capacity Building in Global Economics* (pp. 315–330). IGI Global. https://doi.org/10.4018/978-1-6684-6766-4.ch017

Few, S., Barton, J., Sandwell, P., Mori, R., Kulkarni, P., Thomson, M., Nelson, J., & Candelise, C. (2022). Electricity demand in populations gaining access: Impact of rurality and climatic conditions, and implications for microgrid design. *Energy for Sustainable Development, 66*, 151–164. https://doi.org/10.1016/j.esd.2021.11.008

Fotis, G., Dikeakos, C., Zafeiropoulos, E., Pappas, S., & Vita, V. (2022). Scalability and replicability for smart grid innovation projects and the improvement of renewable energy sources exploitation: The Flexitranstore case. *Energies, 15*, 4519. https://doi.org/10.3390/en15134519

Goel, S., & Sharma, R. (2019). Optimal sizing of a biomass–biogas hybrid system for sustainable power supply to a commercial agricultural farm in northern Odisha, India. *Environment, Development and Sustainability, 21*(5), 2297–2319.

Gökçek, M. (2018). Integration of hybrid power (wind-photovoltaic-diesel-battery) and seawater reverse osmosis systems for small-scale desalination applications. *Desalination, 435*, 210–220. https://doi.org/10.1016/j.desal.2017.07.006

Government of India. Ministry of new and renewable energy;2020–21. <http://mnre.gov.in/schemes/grid-connected/solar/. Accessed 5 Dec 2021

Hafez, A. A., Nassar, Y. F., Hammdan, M. I., & Alsadi, S. Y. (2020). Technical and economic feasibility of utility-scale solar energy conversion systems in Saudi Arabia. *Iranian Journal of Science and Technology, Transactions of Electrical Engineering, 44*, 213–225. https://doi.org/10.1007/s40998-019-00233-3

International Energy Agency (IEA). Global shifts in the energy system in world energy outlook 2017. Paris: International Energy Agency, 14 Nov 2017.

Jahn U., Mayer, D., Heidenreich, M., Dahl, R., Castello, S., Clavadetscher, L., Frölich, A., Grimmig, B., Nasse, W., Sakuta, K. and Sugiura, T., 2000, May. International Energy Agency PVPS Task 2: Analysis of the operational performance of the IEA Database PV systems. In *16th european photovoltaic solar energy conference and exhibition, Glasgow, United Kingdom* (p 5).

Jed, M. E. H., Ihaddadene, R., Ihaddadene, N., Sidi, C. E. E., & Bah, M. E. (2020). Performance analysis of 954,809 kWp PV array of Sheikh Zayed solar power plant (Nouakchott, Mauritania). *Renewable Energy Focus, 32*, 45–54. https://doi.org/10.1016/j.ref.2019.11.002

Jeyasudha, S., Krishnamoorthy, M., Saisandeep, M., Balasubramanian, K., Srinivasan, S. and Thaniaknti, S.B., 2021 Techno economic performance analysis of hybrid renewable electrification system for remote villages of India. *International Transactions on Electrical Energy Systems 31*(10). https://doi.org/10.1002/2050-7038.12515

Kabeel, A. E., Abdelgaied, M., & Sathyamurthy, R. (2019). A comprehensive investigation of the optimization cooling technique for improving the performance of PV module with reflectors under Egyptian conditions. *Solar Energy, 186*, 257–263. https://doi.org/10.1016/j.solener.2019.05.019

Kazem, H. A., Al-Badi, H. A., Al Busaidi, A. S., & Chaichan, M. T. (2017). Optimum design and evaluation of hybrid solar/wind/diesel power system for Masirah Island. *Environment, Development and Sustainability, 19*(5), 1761–1778. https://doi.org/10.1007/s10668-016-9828-1

Kazem, H. A., & Khatib, T. (2013). Techno-economical assessment of grid-connected photovoltaic power systems productivity in Sohar, Oman. *Sustainable Energy Technologies and Assessments, 3*, 61–65. https://doi.org/10.1016/j.seta.2013.06.002

Kumar, P., Sikder, P. S., & Pal, N. (2018). Biomass fuel cell based distributed generation system for Sagar Island. *Bulletin of the Polish Academy of Sciences. Technical Sciences*. https://doi.org/10.24425/bpas.2018.124282

Kumar, J., & Kumar, N. (2022). Optimal Scheduling of grid connected solar photovoltaic and battery storage system considering degradation cost of battery. *Iranian Journal of Science and Technology, Transactions of Electrical Engineering, 46*(4), 1175–1188. https://doi.org/10.1007/s40998-022-00529-x

Kumar, J., Suryakiran, B. V., Verma, A., & Bhatti, T. S. (2019). Analysis of techno-economic viability with demand response strategy of a grid-connected microgrid model for enhanced rural electrification in Uttar Pradesh state, India. *Energy, 1*(178), 176–185. https://doi.org/10.1016/j.energy.2019.04.105

Kumar, P., Kumar, M., & Pal, N. (2021a). AN efficient control approach OF voltage and frequency regulation IN an autonomous microgrid. *Revue Roumaine Des Sciences Techniques-Serie Electrotechnique Et Energetique, 66*(1), 33–39.

Kumar, P., Pal, N., & Sharma, H. (2020). Performance analysis and evaluation of 10 kWp solar photovoltaic arrays for remote islands of Andaman and Nicobar. *Sustainable Energy Technologies and Assessments, 42*, 100889. https://doi.org/10.1016/j.seta.2020.100889

Kumar, P., Pal, N., & Sharma, H. (2021b). Techno-economic analysis of solar photo-voltaic/diesel generator hybrid system using different energy storage technologies for isolated islands of India. *Journal of Energy Storage, 41*, 102965. https://doi.org/10.1016/j.est.2021.102965

Kumar, P., Pal, N., & Sharma, H. (2022). Optimization and techno-economic analysis of a solar photovoltaic/biomass/diesel/battery hybrid off-grid power generation system for rural remote electrification in eastern India. *Energy*. https://doi.org/10.1016/j.energy.2022.123560

Kymakis, E., Kalykakis, S., & Papazoglou, T. M. (2009). Performance analysis of a grid-connected photovoltaic park on the island of Crete. *Energy Conversion and Management, 50*(3), 433–438. https://doi.org/10.1016/j.enconman.2008.12.009

Li, J., Liu, P., & Li, Z. (2020). Optimal design and techno-economic analysis of a solar-wind-biomass off-grid hybrid power system for remote rural electrification: A case study of west China. *Energy, 208*, 118387. https://doi.org/10.1016/j.energy.2020.118387

Lilienthal P. How HOMER calculates PV output power, Wind turbine power and battery output, energy charge output, total net present cost, Cost of energy and break-even grid extension distance, homer help file 2016. HOMER® Pro Version 3.7 User Manual; August 2016. http://homerenergy.com/. Accessed 11 Nov 2021.

Lilienthal P. Autosize Genset diesel generator, Homer Pro software user manual. HOMER® Pro Version 3.7 User Manual; August 2016. https://www.homerenergy.com/products/pro/docs/latest/index.html/. Accessed 7 Nov 2021.

Ma, T., Yang, H., & Lu, L. (2013). Performance evaluation of a stand-alone photovoltaic system on an isolated island in Hong Kong. *Applied Energy, 112*, 663–672. https://doi.org/10.1016/j.apenergy.2012.12.004

Malvoni, M., Leggieri, A., Maggiotto, G., Congedo, P. M., & De Giorgi, M. G. (2017). Long term performance, losses and efficiency analysis of a 960 kWP photovoltaic system in the Mediterranean climate. *Energy Conversion and Management, 145*, 169–181. https://doi.org/10.1016/j.enconman.2017.04.075

Mehta, S. and Basak, P., 2020, February. A case study on pv assisted microgrid using homer pro for variation of solar irradiance affecting cost of energy. In *2020 IEEE 9th power india international conference (PIICON)* (pp. 1–6). IEEE. https://doi.org/10.1109/PIICON49524.2020.9112894.

Miao, C., Teng, K., Wang, Y., & Jiang, L. (2020). Technoeconomic analysis on a hybrid power system for the UK household using renewable energy: a case study. *Energies, 13*(12), 3231. https://doi.org/10.3390/en13123231

Ministry of Housing and Urban Affairs. https://smartcities.gov.in/. Accessed 19 Oct 2023

Ministry of Petroleum & Natural Gas. Pradhan Mantri ujjwalayojna http://petroleum.nic.in/. Accessed 15 Oct 2023

Ministry of New and Renewable Energy. https://mnre.gov.in/policies-and-regulations/schemes-and-guidelines/schemes/. Accessed 30 Oct 2023

Ministry of New and Renewable Energy, Initiatives & achievements, Gov. India. (2020–21). https://mnre.gov.in/ Accessed 19 Nov 2021

MNRE Annual Report 2020_Changes file_18.03. 201.indd. https://mnre.gov.in/img/documents/uploads/file_f-1618564141288.pdf/. Accessed 19 Dec 2021

Mondol, J. D., Yohanis, Y., Smyth, M., & Norton, B. (2006). Long term performance analysis of a grid connected photovoltaic system in Northern Ireland. *Energy Conversion and Management, 47*(18–19), 2925–2947. https://doi.org/10.1016/j.enconman.2006.03.026

Mpholo, M., Nchaba, T., & Monese, M. (2015). Yield and performance analysis of the first grid-connected solar farm at Moshoeshoe I International Airport, Lesotho. *Renewable Energy, 81*, 845–852. https://doi.org/10.1016/j.renene.2015.04.001

Multiple data access option, National Aeronautics and Space Administration (NASA): 2021. https://power.larc.nasa.gov/. Accessed 22 Oct 2021

Nassar, Y. F., Alsadi, S. Y., El-Khozondar, H. J., Ismail, M. S., Al-Maghalseh, M., Khatib, T., Saed, J. A., Mushtaha, M. H., & Djerafi, T. (2022). Design of an isolated renewable hybrid energy system: a case study. *Materials for Renewable and Sustainable Energy, 11*(3), 225–240. https://doi.org/10.1007/s40243-022-00216-1

Odou, O. D. T., Bhandari, R., & Adamou, R. (2020). Hybrid off-grid renewable power system for sustainable rural electrification in Benin. *Renewable Energy, 145*, 1266–1279. https://doi.org/10.1016/j.renene.2019.06.032

Padmavathi, K., & Daniel, S. A. (2013). Performance analysis of a 3 MWp grid connected solar photovoltaic power plant in India. *Energy for Sustainable Development, 17*(6), 615–625. https://doi.org/10.1016/j.esd.2013.09.002

Pawar, N. and Nema, P., 2018 Techno-economic performance analysis of grid connected PV solar power generation system using HOMER software. In *2018 IEEE International Conference on Computational Intelligence and Computing Research (ICCIC)* (PP. 1–5). IEEE. https://doi.org/10.1109/ICCIC.2018.8782411.

Pietruszko, S. M., & Gradzki, M. (2003). Performance of a grid connected small PV system in Poland. *Applied Energy, 74*(1–2), 177–184. https://doi.org/10.1016/S0306-2619(02)00144-7

PM-KUSUM (Pradhan Mantri Kisan Urja Suraksha evamUtthaanMahabhiyan) Scheme. < https://www.india.gov.in/spotlight/pm-kusum-pradhan-mantri-kisan-urja-suraksha-evam-utthaan-mahabhiyan-scheme>. Accessed 11 Oct 2023

Power scenario in West Bengal. <https://wbpower.gov.in/power-scenario-in-west-bengal/>. Accessed 18 Sep 2023

Power for All West Bengal. <https://powermin.gov.in/sites/default/files/uploads/joint_initiative_of_govt_of_india_and_West_Bengol.pdf>. Accessed 27 Sep 2023

Press Information Bureau. <https://pib.gov.in/PressReleseDetailm.aspx?PRID=1907700>. Accessed 3 Nov 2023.

Press Information Bureau. <www.pib.gov.in>. Accessed 25 Oct 2023.

Pujari, H. K., & Rudramoorthy, M. (2021). Optimal design and techno-economic analysis of a hybrid grid-independent renewable energy system for a rural community. *International Transactions on Electrical Energy Systems, 31*(9), e13007. https://doi.org/10.1002/2050-7038.13007

Quansah, D. A., Adaramola, M. S., Appiah, G. K., & Edwin, I. A. (2017). Performance analysis of different grid-connected solar photovoltaic (PV) system technologies with a combined capacity of 20 kW in a humid tropical climate. *International Journal of Hydrogen Energy, 42*(7), 4626–4635. https://doi.org/10.1016/j.ijhydene.2016.10.119

Rahman, M. M., Hasan, M. M., Paatero, J. V., & Lahdelma, R. (2014). Hybrid application of biogas and solar resources to fulfill household energy needs: A potentially viable option in rural areas of developing countries. *Renewable Energy, 68*, 35–45. https://doi.org/10.1016/j.renene.2014.01.030

Saiprasad, N., Kalam, A. and Zayegh, A., 2018. Comparative study of optimization of HRES using HOMER and iHOGASoftware. http://nopr.niscair.res.in/handle/123456789/45489

Salameh, T., Ghenai, C., Merabet, A., & Alkasrawi, M. (2020). Techno-economical optimization of an integrated stand-alone hybrid solar PV tracking and diesel generator power system in Khorfakkan. *United Arab Emirates. Energy, 190*, 116475. https://doi.org/10.1016/j.energy.2019.116475

Salehin, S., Ferdaous, M. T., Chowdhury, R. M., Shithi, S. S., Rofi, M. B., & Mohammed, M. A. (2016). Assessment of renewable energy systems combining techno-economic optimization with energy scenario analysis. *Energy, 112*, 729–741. https://doi.org/10.1016/j.energy.2016.06.110

Sambhi, S., Sharma, H., Bhadoria, V., Kumar, P., Chaurasia, R., Chaurasia, G. S., Fotis, G., Vita, V., Ekonomou, L., & Pavlatos, C. (2022a). Economic feasibility of a renewable integrated hybrid power generation system for a rural village of Ladakh. *Energies, 15*(23), 9126. https://doi.org/10.3390/en15239126

Sambhi, S., Sharma, H., Bhadoria, V., Kumar, P., Fotis, G., & Ekonomou, L. (2023). Technical and 2E Analysis of Hybrid Energy Generating System with Hydrogen Production for SRM IST Delhi-NCR Campus. *Designs, 7*(2), 55. https://doi.org/10.3390/designs7020055

Sambhi, S., Sharma, H., Kumar, P., Fotis, G., Vita, V., & Ekonomou, L. (2022b). Techno-economic optimization of an off-grid hybrid power generation for SRM IST. *Delhi-NCR Campus. Energies, 15*, 7880. https://doi.org/10.3390/en15217880

Sawle, Y., Jain, S., Babu, S., Nair, A. R., & Khan, B. (2021). Prefeasibility economic and sensitivity assessment of hybrid renewable energy system. *IEEE Access, 9*, 28260–28271. https://doi.org/10.1109/ACCESS.2021.3058517

Seme, S., Sredenšek, K., Štumberger, B., & Hadžiselimović, M. (2019). Analysis of the performance of photovoltaic systems in Slovenia. *Solar Energy, 180*, 550–558. https://doi.org/10.1016/j.solener.2019.01.062

Shahzad, M. K., Zahid, A., Ur, R. T., Rehan, M. A., Ali, M., & Ahmad, M. (2017). Techno-economic feasibility analysis of a solar-biomass off grid system for the electrification of remote rural areas in Pakistan using Homer software. *Renewable Energy, 106*, 264–273. https://doi.org/10.1016/j.renene.2017.01.033

Sharma, R., & Goel, S. (2016). Stand-alone hybrid energy system for sustainable development in rural India. *Environment, Development and Sustainability, 18*(6), 1601–1614. https://doi.org/10.1007/s10668-015-9705-3

Sharma, V., & Chandel, S. S. (2013). Performance analysis of a 190 kWp grid interactive solar photovoltaic power plant in India. *Energy, 55*, 476–485. https://doi.org/10.1016/j.energy.2013.03.075

Sidrach-de-Cardona, M., & Lopez, L. M. (1999). Performance analysis of a grid-connected photovoltaic system. *Energy, 24*(2), 93–102. https://doi.org/10.1016/S0360-5442(98)00084-X

Sun, H., Awan, R. U., Nawaz, M. A., Mohsin, M., Rasheed, A. K., & Iqbal, N. (2021). Assessing the socio-economic viability of solar commercialization and electrification in south Asian countries. *Environment Development and Sustainability, 23*(7), 9875–9897. https://doi.org/10.1007/s10668-020-01038-9

Sundaram, S., & Babu, J. S. C. (2015). Performance evaluation and validation of 5 MWp grid connected solar photovoltaic plant in South India. *Energy Conversion and Management, 100*, 429–439. https://doi.org/10.1016/j.enconman.2015.04.069

Tarhan, S., & Sarı, A. (2005). Model selection for global and diffuse radiation over the Central Black Sea (CBS) region of Turkey. *Energy Conversion and Management, 46*(4), 605–613. https://doi.org/10.1016/j.enconman.2004.04.004

Thotakura, S., Kondamudi, S. C., Xavier, J. F., Quanjin, M., Reddy, G. R., Gangwar, P., & Davuluri, S. L. (2020). Operational performance of megawatt-scale grid integrated rooftop solar PV system in India's tropical wet and dry climates. *Case Studies in Thermal Engineering, 18*, 100602. https://doi.org/10.1016/j.csite.2020.100602

Vendoti, S., Muralidhar, M., & Kiranmayi, R. (2021). Techno-economic analysis of off-grid solar/wind/biogas/biomass/fuel cell/battery system for electrification in a cluster of villages by HOMER software. *Environment, Development and Sustainability, 23*(1), 351–372. https://doi.org/10.1007/s10668-019-00583-2

Vivas Fernández, F. J., Heras Jiménez, A. D. L., Segura Manzano, F., & Andújar Márquez, J. M. (2018). A review of energy management strategies for renewable hybrid energy systems with hydrogen backup. *Renewable and Sustainable Energy Reviews, 82*, 126–155. https://doi.org/10.1016/j.rser.2017.09.014

Yao, W., Li, Z., Wang, Y., Jiang, F., & Hu, L. (2014). Evaluation of global solar radiation models for Shanghai, China. *Energy Conversión and Management, 84*, 597–612. https://doi.org/10.1016/j.enconman.2014.04.017

Publisher's Note Springer Nature remains neutral with regard to jurisdictional claims in published maps and institutional affiliations.

Springer Nature or its licensor (e.g. a society or other partner) holds exclusive rights to this article under a publishing agreement with the author(s) or other rightsholder(s); author self-archiving of the accepted manuscript version of this article is solely governed by the terms of such publishing agreement and applicable law.